Theory of Electron Spin Resonance in Low Dimensional Quantum Magnets

Department of Physics, Graduate School of Science, Osaka University

Taro Yoshino[1]

February, 1999

[1]E-mail: taro@godzilla.phys.sci.osaka-u.ac.jp

Contents

Chapter 1

Introduction

1.1 At the beginning

When we study various materials, we often use the method in which we apply a field to material and observe the response. ESR, electron spin resonance is a typical one. We give the static magnetic field and an oscillating field to the material and observe absorption, which is described by complex susceptibility $\chi''(\omega)$[1]. Electron spin resonance method has been a very powerful tool to study the energy structure of the material, from which we can reduce hamiltonian of the material to to determine hamiltonian.

Turning our eye to the quantum spin system, after the Haldane conjecture in 1983[2, 3],there are many studies on the low dimensional quantum spin system, which reveals that "non-magnetic" material in conventional sense has various quantum phases in the grand states. There, the singlet pair(valance bond) plays as a freedom of system and its various spatial configuration describes the characteristics of the distinguishable quantum phases in the ground states.

For example, AKLT model, a model of the $S = 1$ of one dimensional quantum spin system (see section 1.2.4), shows a disordered state so called "quantum liquid" in the ground states. There, existence of energy gap and the exponentially decaying spin-spin

correlation function has proved. A new type of quantum order so called hidden order has been

also pointed out [33, 34].

With combination of various experiments on the quasi-one dimensional materials and various numerical experiments, knowledge of the low dimensional quantum spin system has been extremely improved.

On the other hand, surveying the theories on electron spin resonance, only few works have taken into account the quantum many-body effect. Nothing to say that there are no need to take into account the many-body effect in analyzing the paramagnetic resonance, because each spin resonates individually. In the ferromagnetic resonance case and the anti-ferromagnetic case, system have been treated as a classical vector.

Among them, Nagata-Tazuke's theory is notable. Using Kanamori-Tachiki's formalism [6] and explicit expression of the spin-spin correlation function in one dimensional classical spin system, they made a good reproduction of the temperature dependence of resonance shift comparing with experimental results of $CsMnCl_3 \cdot 2H_2O$.

In recent years, electron spin resonance experiments on various quasi-one dimensional material attracts interests[30, 29, 26]. The system thought in some disordered quantum phases. But there are no theory of electron spin resonance which gives the physical perspective on such a quantum disordered system in which spin-spin correlation plays essential role and the system has no long range order.

To investigate the electron spin resonance in such a strongly fluctuating quantum system, we proposed a direct numerical method [4] to calculate the dynamical susceptibility $\chi''(\omega)$ via Kubo-formula [8, 9]. We calculate the spin-spin correlation function numerically exact on the quantum system and apply the Kubo formula. So we can obtain the exact absorption line shape and the g value shift originated anisotropic effect of exchange integral, dipole-dipole interaction and the Dzyaloshinsky-Moriya interaction.

Using this method, we can adopt the geometrical effect of the system exactly, *i.e.*, dipole-dipole interaction effect originated from

the system spatial structure, effect of configuration of the static magnetic field and oscillating magnetic field to the system. Therefore, we can obtain the absorption line shape for an actual material[4]. We studied relevant model for the experiments, such that bond alternating one dimensional zigzag chain[5]. We also estimate effect of the Dzyaloshinsky-Moriya interaction effect for resonance[5]. Furthermore, we studied electron spin resonance in the systems which have various quantum phases in its ground states.

Especially, we paid attention to the dynamical shift, *i.e.* the geometry configuration dependence of a resonance shift, the shift from paramagnetic resonance frequency. We regards the dynamical shift is one of the important quantities which reveal the nature of the system via ESR. We propose that we can determine exchange integrals which no other macroscopic measurement can determine until now

comparing the dynamical shift both numerically and experimentally[5].

In computer physics, it is required to understand physical characteristics of the system effectively within the computer capacity. Computer simulation is one of the most powerful method to investigate the physics of the system for which explicit theory can not be available. Until now, no definitive theory of electron spin resonance on low dimensional quantum magnets. So we hope that direct calculation of dynamical shift of the system is beneficial to the theoretical understandings of ESR. We strongly hope that this thesis would clarify the field where combination of numerical experiments and ESR measurement will be able to determine various nature of material.

In chapter 1, we introduce the perspective of this thesis in the first section. After that, we review the general property of low dimensional quantum spin systems. The ground state phase diagram of bond alternating chain will be reviewed.

In chapter 2, we survey the theory of electron spin resonance. Classical description, one electron case, phenomenological theory with relaxation, paramagnetic resonance theory will be explained. After that we survey Nagata-Tazuke's theory which considers many-body effect. At the last section, we explain the detailed procedure how to obtain the absorption line shape via Kubo formula. We note a perturbation treatment of Kubo formula and the theory with dissipation effect.

In chapter 3, we explain the method that direct calculation of the complex susceptibility via Kubo formula. In first section, we show the background why we need this method. After that, practical procedure to perform the calculation with computer is presented.

In chapter 4, we analyze one dimensional antiferromagnetic Heisenberg chain using the method which we introduced in chapter 3, with attention to the dynamical shift. First, we show our method is a appropriate method. After that, we investigate change of the resonance in various geometrical configuration of the system. The effects of the static field strength, oscillation field strength, and anisotropy dependence of the sift of resonance are also studied.

In chapter 5, we apply our method to the chain with zigzag space structure. The system is ferromagnetic-antiferromagnetic bond alternating chain with anisotropy, which is the relevant model to $Cu_{0.9}Zn_{0.1}Nb_2O_6$. We show the importance of system anisotropy.

In chapter 6, we show the possibility that we can determine the system constants, *i.e.*, which bond is ferromagnetic and which bond is antiferromagnetic, using the dynamical shift both from our simulation and from experiments.

In chapter 7, we investigate the dynamical shift in the bond alternating chain in various quantum phases. Chapter 8 is devoted to summary and discussion. Chapter 9 is for acknowledgment. At the end of this thesis, appendices are attached.

1.2 Upon low dimensional quantum spin system

1.2.1 Basic properties of the quantum spin

Insulator's magnetism is carried by the magnetic moment of electrons which are localized at the atoms on lattice. Assuming there are n electrons carrying magnetism in an atom, composition of the spins $n/2$, due to the Hund rule.

If we can consider the spins are localized to the lattice, we call the system as spin system.

Due to the overlap of the wave functions, the exchange interactions between spins appear. Arrangements of exchange interactions determine various forms of quantum spin systems.

Adding to the exchange interaction, there are the dipole-dipole interaction between any two spins in the lattice. Due to the system asymmetricity, there is the Dzyaloshinsky-Moriya interaction[24, 25] between nearest neighbor spins. This interaction is antisymmetric with

spin exchange. These interactions cause the shift in the electron spin resonance measurement. So these interactions are important in electron spin resonance. They supply small effect to the quantum phases nature because the amplitude of them are small comparing the exchange interaction.

Each component of a quantum spin $\mathbf{S}$, *i.e.* S^x, S^y, and S^z, satisfies following relations.

$$[S^x, S^y] = i\hbar S^z, [S^y, S^z] = i\hbar S^x, [S^z, S^x] = i\hbar S^y, \tag{1.1}$$

where $\hbar$ denotes $h/2\pi$ (h denotes the Plank constants). We set $\hbar = 1$ here. The magnitude of the spin, S denotes as

$$\mathbf{S}^2 = S(S+1).$$

If S is equal to $\frac{1}{2}$, we can represent S^x, S^y and S^z using the Pauli matrix σ as follows.

$$\sigma^x = \begin{pmatrix} 0 & 1 \\ 1 & 0 \end{pmatrix}, \sigma^y = \begin{pmatrix} 0 & -i \\ i & 0 \end{pmatrix}, \sigma^z = \begin{pmatrix} 1 & 0 \\ 0 & -1 \end{pmatrix}, \tag{1.2}$$

$$S^x = \frac{1}{2}\sigma^x, S^y = \frac{1}{2}\sigma^y, S^z = \frac{1}{2}\sigma^z. \tag{1.3}$$

With the commutation relation shown as Eq. (1.1), the quantum spin system shows various characteristics which we can not see in the classical spin system.

We will explain the exchange interaction. If two spins ($\mathbf{S}_1\mathbf{S}_2$) interacts with exchange interaction, the system hamiltonian described as

$$\mathcal{H} = 2J\mathbf{S}_1\mathbf{S}_2. \tag{1.4}$$

We call this interaction exchange interaction. If J is negative, *i.e.* the energy of the system is minimized when two spin's directions are the same, we call the bond ferromagnetic. If J is positive, *i.e.* the energy of the system is minimized when two spin's directions are different, we call the bond antiferromagnetic. Furthermore, if the static magnetic field H is applied to the system, Zeeman term is added to the system hamiltonian. Zeeman term is described as

$$\mathcal{H}_{zeeman} = -H(S_1^z + S_2^z). \tag{1.5}$$

1.2.2 The order of Heisenberg spin system

In the classical antiferromagnetic Heisenberg spin system, it's ground state is the Néel state. We can describe the Néel state as an arrangement of spin states up, down, up, down, alternatively.

It is not obvious in the quantum spin case because the Néel state is not the ground state. Here we summarize the system dimension dependence and temperature dependence of the order. Below, T denotes the temperature.

3 dimensional system

- $T_c \neq 0$. Phase transition occurs at a finite temperature.

2 dimensional system

- At $T = 0$, the long range order exists[12, 11].
- At $T > 0$, no long range order[10] exists.

1 dimensional system

$S = 1/2$ At $T = 0$, the spin-spin correlation function decays by a power as $\propto L^{-\eta}$. No long range order at $T = 0$.

$S = 1$ At $T = 0$,the spin-spin correlation function decays exponentially as $\propto \mathrm{e}^{-\gamma L}$. No long range order at $T = 0$.

1.2.3 Theory and properties of the Haldane system

Here, we review the properties of a one dimensional $S = 1$ antiferro magnetic spin system, called "Haldane system".

The Haldane conjecture

At 1983, Haldane presented the conjecture about one dimensional quantum spin systems, *i.e.*, half odd integer spin system , $S = 1/2S = 3/2S = 5/2 \cdots$ and integer spin system has essentially different properties in the ground states.

The conjecture described as follows.

- Integer spin case
  - The Ground state is rotationally symmetric and only one.
  - There **exists an finite energy gap** between the ground state and the first excited state.
  - Spin-spin correlation function **decays exponentially** in the ground state.
- Half odd integer spin case
  - The ground state is rotationally symmetric and only one.
  - There **exists no energy gap** between the ground state and the first excited state.
  - Spin-spin correlation function **decays by a power** in the ground state.

Until the Haldane conjecture, it is believed that in quantum spin systems of general spin also have this half odd integer spin characteristic. It is believed that we can make the first excited state with state using spin wave with infinitesimal small wave number k, and believed that this state is orthogonal to the ground state. So this integer spin behavior changed the "common sense". Now, with various numerical study, theoretical study, and experiments, Haldane's conjecture is considered to be true. We call the system in which the Haldane's conjecture holds the Haldane system. The typical one is $S = 1$ one dimensional antiferromagnetic Heisenberg chain.

1.2.4 AKLT model

To understand the nature of the ground state of the Haldane system, we often uses the picture that valence bond (spin singlet pair) covers the system and moves around.

For the system consists of two $S = 1/2$ spins interacting antiferro-magnetically, the ground states is shown as

$$\frac{1}{2}(|\uparrow\rangle_1|\downarrow\rangle_2 - |\downarrow\rangle_1|\uparrow\rangle_2), \tag{1.6}$$

we call this state spin singlet state or singlet pair. This state is rotationally symmetric and the expectation value of $S_1^z + S_2^z$ becomes 0. We call this states as valance bond.

We call such systems "quantum liquid".

AKLT model is given as

$$\mathcal{H} = J\sum_i^N(\mathbf{S}_i\mathbf{S}_{i+1} + \frac{1}{3}(\mathbf{S}_i\mathbf{S}_{i+1})^2), \tag{1.7}$$

where $J > 0$.

It has been proved that if the model has the ground state which can describe as valence bonds cover the system. It is proved that Haldane's conjecture holds explicitly in AKLT model[33].

1.2.5 Various phases in the ground state

We can add the single-ion anisotropy D term to the $S = 1$ one dimensional Heisenberg model:

$$\mathcal{H}_{\mathcal{LD}} = \sum_i J\mathbf{S}_i\mathbf{S}_{i+1} + D(S_i^z)^2. \tag{1.8}$$

If D is 0, we call the system is in the Haldane phase in the ground state. If D is sufficiently big comparing J (> 0), the system is in the so called large D phase.

Here, we introduce two order parameters described by spin-spin correlation.

We introduce Néel order parameter as

$$O_{N\acute{e}el} = \lim_{|i-j|\to\infty}(-1)^{(i-j)}\langle GS|\mathbf{S}_i\mathbf{S}_j|GS\rangle. \tag{1.9}$$

If this order parameter is finite, the system has Néel order. We also say the system is in Néel phase. The classical antiferromagnetic spin system has Néel order in the ground state. But no Néel order in the Haldane phase and in the large D phase. This means that the ground state of the Haldane system has different nature from that in the classical spin system case.

To distinguish the Haldane phase and the large D phase, we introduce the string order parameter as

$$O_{string} = -\lim_{j-i\to\infty} \langle GS|S_i^\alpha e^{i\pi\sum_{k=i+1}^{j-1} S_k^\alpha} S_j^\alpha|GS\rangle. \tag{1.10}$$

Here, $\alpha = x$, y or z. In Haldane phase, this order parameter is finite and in large D phase, this order parameter vanishes.

The spin state of the system is described as $\cdots + -0 + -0 + 0 - + - \ldots$. Finite string order parameter means that the system has Néel order if we ignore the spins in the state 0. This order is isotropic, *i.e.* we can confirm this order from any direction[34]. Because we can not detect this order experimentally, we call this order as "hidden order". We can "see" this order in computer simulation.

Phase transition between Haldane phase and Dimer phase has found in $S = 1$ one dimensional antiferromagnetic bond alternating chain in the ground state by Kato-Tanaka[15]. This phase transition beaks $Z_2 \times Z_2$ symmetry. We set system hamiltonian as

$$\mathcal{H} = \sum_{i=1}^{N_S-1} (1 - (-1)^i\delta)\mathbf{S}_i\mathbf{S}_{i+1}. \tag{1.11}$$

Case $\delta = 0$, the system is Haldane system, and case $\delta = 1$, the system is in "Dimer phase" in the ground state. Dimer phase is described with a picture two valence bonds at the strong bond and no valence bond at the weak bond. They studied the gap between the ground state and the first excited state when δ changes 0 to 1, as Fig 2. Between dimer phase and Haldane phase, there is a point where the gap vanishes. Similar phase transition occurs in $S = 2$ case[16].

1.3 The phase diagram of $S = 1/2$ bond alternating Heisenberg chain in the ground state

In this section, we summarize the phase diagram of the $S = 1/2$ bond alternating Heisenberg chain obtained by Hida[18, 19]. There the bond strength of the system changes ferromagnetic-antiferromagnetic alternatively. Effect of anisotropy is also considered.

We set the hamiltonian of $S = 1/2$ bond alternating spin chain as

$$\mathcal{H} = \sum_i^N 2J(S_{2i}^x S_{2i+1}^x + S_{2i}^y S_{2i+1}^y + \lambda S_{2i}^z S_{2i+1}^z) + 2J'\mathbf{S}_{2i-1}\mathbf{S}_{2i} + D(S_{2i-1}^z + S_{2i}^z)^2. \tag{1.12}$$

$\mathbf{S}$ denotes $S = 1/2$ spin operator, N denotes the number of spin in the system, and assume $\mathbf{S}_N = \mathbf{S}_1$, the periodic boundary condition. The ratio $-J'/J$ is denotes by β. λ denotes an anisotropy of antiferromagnetic bond.

For example, if we consider the case $\beta \to \infty$, the system is equivalent to $S = 1$ one dimensional antiferromagnetic with exchange interaction $J_{AF} = 1/2J$, because we can regard the $S = 1/2$ spins besides ferromagnetic bond as one $S = 1$ spin. Other various quantum phases with various parameter has studied[18, 19]. In Fig. 3, the phase diagram is presented.

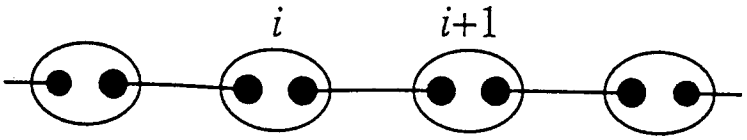

Fig. 1: A rough sketch of Valence Bond Solid state, from [17]. The connected two black painted out circles denotes spin singlet pair (valence bond) and an oval enclosing two black painted out circles denotes a $S = 1$ spin. This oval represents operation of "symmetrize", which can be described as $1/2($ -• •- $+$  $)$.

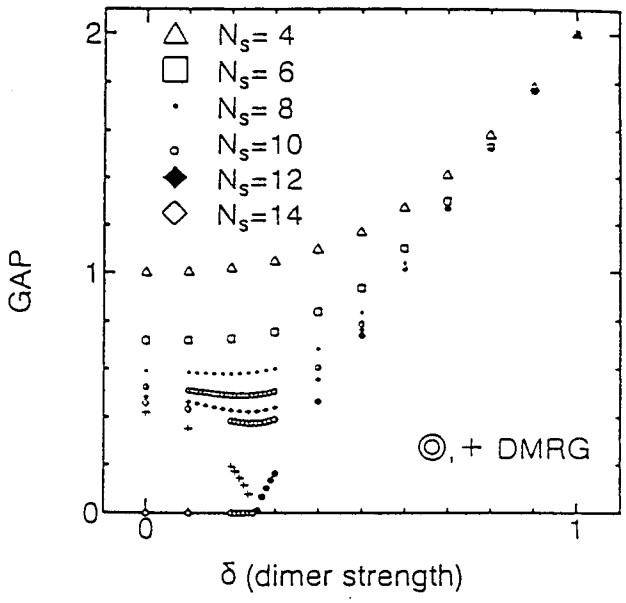

Fig. 2: The gap between the ground state and the first exited states is shown in a horizontal axis. Quotation From [15]. The parameter Δ is shown in a vertical axis. We can see the phase transition at around $\Delta = 0.25$.

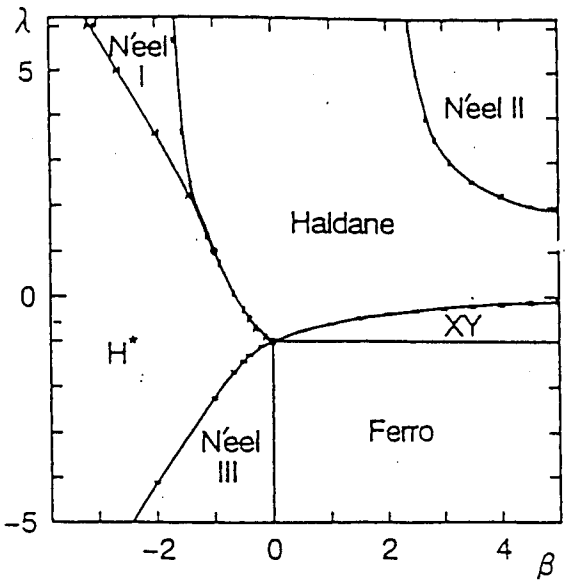

Phase diagram of ALHC with $D = 0$.

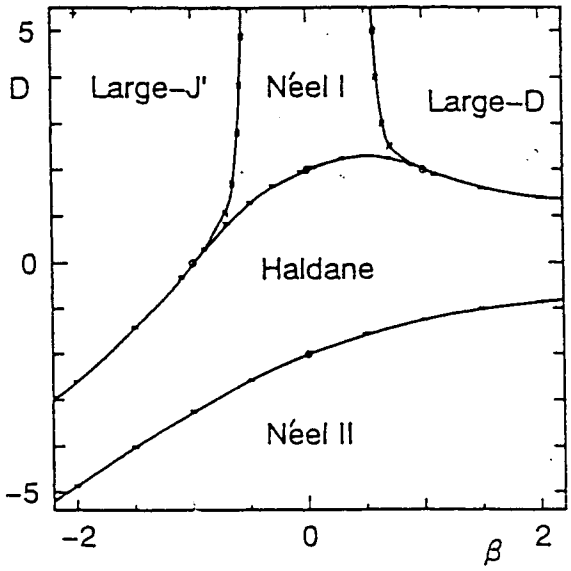

Phase diagram of ALHC with $\lambda = 1$.

Fig. 3: The phase diagram of the $S = 1/2$ bond alternating chain in the ground state. Quotation from [19]. See the text for D and λ 's notation.

Chapter 2

A Brief Review on Theories of Electron Spin Resonance

Until now, there are various theoretical approaches to electron spin resonance. We will present a brief review in this chapter.

We begin with the dynamics of magnets introducuing the Bloch

equation which includes relaxation effect of disipation. We then explain the general idea of the paramagnetic resonance.

After that, we show the fact that if the spin-spin interaction is isotropic (*i.e.*, SU(2) symmetric) then no resonance frequency shift from that of the paramagnetic resonance exists. So if we want to observe the shift, we needs the non-isotropic spin-spin interaction such as the anisotropic coupling, the dipole-dipole interaction, and Dzyaloshinsky-Moriya interaction.

We introduce the Nagata-Tazuke's workwhere they show the resonance shift from paramagnetic case in the one dimensional Heisenberg spin chain with

the dipole-dipole interaction, making use of Kanamori-Tachiki's equation.

We show a derivation of the imaginary part of the susceptibility from the Kubo formula, and derive an exlicite expression for numerical calculations. We also introduce the result of Natsume *et.al.*. They performed a perturbation expansion of Kubo formula and showed dependence of the resonance shift on the angular between the chain ands the static field. At ending, we note the treatment of Hamano *et al.* for a time evolution with a disipation dynamics.

2.1 Larmor rotation

We set $\mathbf{M}$ denotes a magnet, $\mathbf{H}_0$ the static magnetic field.

The classical torque equation is

$$\frac{\mathrm{d}\mathbf{M}}{\mathrm{d}t} = \gamma \left[\mathbf{M} \times \mathbf{H}_0\right]. \tag{2.1}$$

This equation is derived in scope of electrodynamics. γ denotes the gyromagnetic ratio.

Setting $\mathbf{H}_0 = (0, 0, H_z)$, $H_z > 0$, the torque equation is expressed as

$$\frac{\mathrm{d}M^x}{\mathrm{d}t} = \gamma M^y H_z, \ \frac{\mathrm{d}M^y}{\mathrm{d}t} = -\gamma M^x H_z, \ \frac{\mathrm{d}M^z}{\mathrm{d}t} = 0. \tag{2.2}$$

Substituting time differential of the first equation to the second equation, we obtain

$$\frac{\mathrm{d}^2 M_x}{\mathrm{d}t^2} = -\gamma^2 H_0^2 M_x and \frac{\mathrm{d}^2 M_y}{\mathrm{d}t^2} = -\gamma^2 H_0^2 M_y. \tag{2.3}$$

M_x and M_y satisfy the equation of the harmonic oscillation equation. From the third equation, M_z appears a constant.

The eigenfrequency ω_0 of M_x and M_y is

$$\omega_0^2 = |\gamma| H_z, \tag{2.4}$$

and we obtain

$$M_x = M_{x0} \mathrm{e}^{i\omega_0 t}, \ M_y = i\frac{\gamma}{|\gamma|} M_{x0} \mathrm{e}^{i\omega_0 t} \ and \ M_z = M_{z0}. \tag{2.5}$$

Both M_x and M_y have the same amplitude, and have the phase difference of $\frac{\pi}{2}$. If γ's sign changes, the direction of rotation will be reversed. This rotation called Larmor rotation (Fig. 4).

2.2 Magnetic moment of electron

We consider one free electron here. The spin has the charge $-e$, mass m_e and spin $\mathbf{S}$. The spin $\mathbf{S}$ has the eigenvalues $\pm\frac{1}{2}$ setting unit to $\hbar = \frac{h}{2\pi}$(h denotes the Plank constant). The spin has it's own magnetic momentum $\mu_\mathbf{s}$,

$$\mu_\mathbf{s} = -g_\mathrm{e} \left(\frac{e\hbar}{2m_\mathrm{e}} \right) \mathbf{S}, \tag{2.6}$$

where

$$\hbar = 1.05459 \times 10^{-34} \ \mathrm{J/S},$$

,

$$e = 1.60219 \times 10^{-19} \ \mathrm{C}.$$

g_e denotes "g-value" of the spin:

$$g_\mathrm{e} = 2.0023193. \tag{2.7}$$

We use SI unit. Setting Bohr magnetron μ_B as

$$\mu_B = \frac{e\hbar}{2m_\mathrm{e}} = 9.27410 \times 10^{-24} \ \mathrm{JT}^{-1}, \tag{2.8}$$

the zeeman energy H_z in the static magnetic field $\mathbf{H}_0$ is given as

$$H_z = -\mu_s \cdot \mathbf{H}_0 = g_\mathrm{e} \mu_B \mathbf{S} \cdot \mathbf{H}_0. \tag{2.9}$$

The gyromagnetic ratio of electron spin, γ, the ratio between magnetic momentum of the electron spin and anguler momentum of the electron spinis, and it is defined as follows.

$$\gamma_{\mathrm{e}} = \frac{-g_{\mathrm{e}}\mu_B S}{\hbar S} = \frac{-g_{\mathrm{e}}e}{2m_{\mathrm{e}}}. \tag{2.10}$$

So, the magnetic moment of a spin is described as

$$\mu_{\mathbf{s}} = \frac{-g_{\mathrm{e}}e\hbar}{2m_{\mathrm{e}}}\mathbf{S} = \gamma_{\mathrm{e}}\hbar\mathbf{S}. \tag{2.11}$$

2.3 Equation of motion of the quantum spin

In this section, we show the classical torque equation Eq. (2.1) holds in quantum spin case.

We set A as a physical quantity, $\mathcal{H}$ as hamiltonian of system, equation of motion becomes

$$i\hbar\frac{\mathrm{d}\mathbf{A}}{\mathrm{d}t} = [\mathbf{A}, \mathcal{H}] = \mathbf{A}\mathcal{H} - \mathcal{H}\mathbf{A}, \tag{2.12}$$

called Heisenberg equation of motion. Here, [,] denotes commutation relations.

We apply this equation of motion to one free electron with static magnetic field $\mathbf{H}_0$. The system hamiltonian is given as

$$\mathcal{H} = -\gamma_{\mathrm{e}}\hbar\mathbf{H}_0\mathbf{S}. \tag{2.13}$$

Substituting this equation to Eq. (2.12), we obtain

$$i\hbar\frac{\mathrm{d}\mathbf{S}}{\mathrm{d}t} = [-\gamma_{\mathrm{e}}\hbar\mathbf{H}_0\mathbf{S}, \mathbf{S}]. \tag{2.14}$$

We set $\mathbf{H}_0 = (H^x, H^y, H^z)$, and obtain

$$\frac{\mathrm{d}S_z}{\mathrm{d}t} = -i\gamma_{\mathrm{e}}[H^x S^x + H^y S^y + H^z S^z] =$$

$$-i\gamma_{\mathrm{e}}[H^x(S^x S^z - S^z S^x) - H^y(S^y S^z - S^z S^y)]. \tag{2.15}$$

For the spin exchange relation Eq. (1.1), Eq. (2.15), derived as follows.

$$\frac{\mathrm{d}S^z}{\mathrm{d}t} = \gamma_{\mathrm{e}}(-H^x S^y + H^y S^x) = \gamma_{\mathrm{e}}[\mathbf{S} \times \mathbf{H}_0]_z. \tag{2.16}$$

x componet and y component become as

$$\frac{\mathrm{d}\mathbf{S}}{\mathrm{d}t} = \gamma_{\mathrm{e}}[\mathbf{S} \times \mathbf{H}_0]. \tag{2.17}$$

Applying the relation $\mu_{\mathbf{s}} = \gamma_{\mathrm{e}}\hbar\mathbf{S}$ after multiplying $\gamma_{\mathrm{e}}\hbar$ to both side of the Eq. (2.17), we obtain

$$\frac{\mathrm{d}\mu_{\mathbf{s}}}{\mathrm{d}t} = \gamma_{\mathrm{e}}[\mu_{\mathbf{s}} \times \mathbf{H_0}]. \tag{2.18}$$

This equation has the same form as Eq. (2.1). In electron case, as $\gamma_e < 0$, and the rotation is illustrated in Fig. 4(b).

This equation of motion of electron spin can solved exactly. Especially, consider the case static magnetic fields $\mathbf{H}_0$ is parallel to z axes, and consider oscillating field $\mathbf{H}_1$ is orthogonal to $\mathbf{H}_0$ and satisfy $\mathbf{H}_1 = \cos(H_0/|\gamma_e|)$. If we set initial conditions as $|1\rangle$ (quantize axe is set z axe) at $t = 0$, the probability of the spin is in $|1\rangle$ and $|-1\rangle$ states becomes

$$P_+ = \cos^2(\gamma_e H_1 t/2),$$

$$P_- = \sin^2(\gamma_e H_1 t/2), \tag{2.19}$$

respectively. We call them Rabi's formula.

2.4 Phenomenological theory of resonance absorption - Bloch equation

The energy from the oscillation field, first excites the Zeeman energy of each spin of the system. After that, the energy transfer to whole spin system via the spin-spin interaction, such as exchange interaction and dipole-dipole interaction. Naturally, the Zeeman energy of each spin also transfers to the lattice via lattice-spin interaction and became thermal energy and also transfers to outside of the system via radiation.

We introduce the Bloch equation as a representative phenomenological theory of resonance absorption

$$\frac{\mathrm{d}M^{x,y}}{\mathrm{d}t} = \gamma[\mathbf{M} \times \mathbf{H}_0]^{x,y} - \frac{M^{x,y}}{T_2}, \tag{2.20}$$

$$\frac{\mathrm{d}M^{z}}{\mathrm{d}t} = \gamma[\mathbf{M} \times \mathbf{H}_0]^{z} - \frac{M^{z} - M^0}{T_1}. \tag{2.21}$$

$\mathbf{M}$ denotes total sum of the system magnetic moment $\sum_i \mathbf{M}_i$. We assume the static magnetic field $\mathbf{H}_0$ is parallel to the z axis, and assume M_0 is the z component of $\mathbf{M}_0$ in the equiribirium.

We set $T_1 = \infty$ and $T_2 \neq 0$. As $T_1 = \infty$, M_z is maintained constants with time evolution, while $M_{x,y}$ will decay to 0. This means that the phase of each spin $M^{x,y}$ becomes randome after long time. Thus, we call T_2 as the phase memory time. Or we sometimes call T_2 as spin-spin relaxation time, because it comes from the spin-spin interaction.

On the other hands, T_1 is the relaxation time for M_z to the equlibrium value M_0. So we sometimes call T_1 spin-lattice relaxation timeere

If we assume $\gamma^2 H_1^2 T_1 T_2 << 1$, the complex susceptibility $\chi(\omega) = \chi'(\omega) - i\chi''(\omega)$ (see 2.9) is derived as

$$\chi'_x(\omega) = \frac{\chi_0 \gamma^2 H_0^2 (\gamma_2 H_0^2 - \omega^2)}{(\gamma^2 H_0^2 - \omega^2)^2 + 4\omega/T_2^2}$$

and

$$\chi_x''(\omega) = \frac{2\chi_0\gamma^2 H_0^2(\omega/T_2)}{(\gamma^2 H_0^2 - \omega^2)^2 + 4\omega/T_2^2}. \tag{2.22}$$

Here, $\chi_0 = M_0/H_0$. The absorption line shape $\chi_x''(\omega)$ described here is called Lorenzian, the half width is $1/T_2$. In the Bloch equation, the width of the absorption line peek exists due to the relaxation term.

2.5 Paramagnetic resonance and equation of Kanamori-Tachiki

We will consider the paramagnetic case, in which we can assume spin-spin interaction is weak and each spin rotates individually. The resonance frequency of each spin are same.

Here, let $\mathbf{S}(t)$ be the total magnetization of the system $\mathbf{S}(t) = \sum \mathbf{S}_i(t)$. We assume one dominant mode

$$\frac{\mathrm{d}S^+}{\mathrm{d}t} = -\mathrm{i}\omega S^+. \tag{2.23}$$

Now, $S^+ \equiv S^x + iS^y$ and $S^- \equiv S^x - iS^y$.

Combining the commutation relation with Eq. (2.23) and

$$i\hbar\frac{\mathrm{d}S^+}{\mathrm{d}t} = [S^+, \mathcal{H}], \tag{2.24}$$

we obtain

$$i\hbar\langle[S^-, \frac{\mathrm{d}S^+}{\mathrm{d}t}]\rangle = \langle[[\mathcal{H}, S^+], S^-]\rangle. \tag{2.25}$$

Finally, we obtain

$$\hbar\omega = \frac{\langle[S^-, [S^+, \mathcal{H}]]\rangle}{2\langle S_z\rangle} \tag{2.26}$$

using $[S^-, S^+] = -2S_z$.

If we assume that the system hamiltonian consists of only the Zeeman term,

$$\mathcal{H} = g_e\mu_B S^z H_0. \tag{2.27}$$

we obtain from Eq.(2.26) as

$$\hbar\omega = g_e\mu_B H_0. \tag{2.28}$$

ω is the frequency of the paramagnetic resonance.

We can also apply Eq.(2.26) to the hamiltonian with spin-spin interaction. Thus we can take into account the effect of spin-spin interaction.

Furthermore, Kanamori-Tachiki[6] also extent Eq.(2.26) to the case of 2 axis anisotropy where the single mode assumption of Eq. (2.23) is not reasonable.

They obtained

$$\hbar\omega = \frac{(\langle[S^x, [S^x, \mathcal{H}]]\rangle\langle[S^y, [S^y, \mathcal{H}]]\rangle)^{\frac{1}{2}}}{\langle S^z\rangle}. \tag{2.29}$$

2.6 ESR in quantum spin system with interaction

2.6.1 The case of interaction has rotational symmetry

We will consider the case where the exchange interaction is isotropic, *i.e.*, $\mathbf{S}_1\mathbf{S}_1$. The system hamiltonian has the form $\mathcal{H}$ becomes as

$$\mathcal{H} = -J\mathcal{H}_{\rm ss} - \mathcal{H}_{\rm zeeman}$$

$$\equiv -J(S_1^x S_2^x + S_1^y S_2^y + S_1^z S_2^z) - H_0 g_e \mu_B (S_1^z + S_2^z). \tag{2.30}$$

Here, the relation

$$[\mathcal{H}_{\rm ss}, S^\alpha] = 0 \tag{2.31}$$

holds with $S^\alpha = S_1^\alpha + S_2^\alpha$, $\alpha = x, y$ and z case. So, applying Eq. (2.26) to this hamiltonian, we obtain the resonance frequency ω as

$$\omega = g\mu_B H_0. \tag{2.32}$$

This is the same frequency comparing from the paramagnetic case, $\mathcal{H} = \mathcal{H}_{\rm zeeman}$. To observe the resonance shift from the paramagnetic resonance, we should take into account the some anisotropy effect in the system hamiltonian, *i.e.*, exchange interaction, anisotropy of the exchange interaction, the dipole-dipole interaction, and the Dzyaloshinsky-Moriya interaction. In the realistic system, g is a tensor. Anisotropy effect of g will also effects to the resonance shift. In other words, the system hamiltonian should breaks the SU(2) symmetry.

2.7 Dipole-dipole interaction and theory of Nagata and Tazuke

As we had see at previous section, the interaction which breaks SU(2) symmetry is needed to observe the resonance shift. Nagata and Tazuke derived the formula of the temperature dependence of the resonance shift in the one dimensional antiferromagnetic chain with dipole-dipole interaction. They succeeded to explain the experimental results of $CsMnCl_3{\cdot}2H_2O$[7].

They start with following interaction,

$$U_d = \sum_{i=0}^{N} \frac{g\mu_B \mathbf{S}_i g\mu_B \mathbf{S}_{i+1}}{r_{i,i+1}^3} - \frac{3(g\mu_B \mathbf{S}_i \mathbf{r}_{i,i+1})(g\mu_B \mathbf{S}_{i+1}\mathbf{r}_{i,i+1})}{r_{i,j}^5}, \tag{2.33}$$

which contains dipole-dipole interaction. Here,the number of spins is $N+1$. $\mathbf{r}_{i,j}$ denotes the vector from the i th lattice to j th lattice. And $r_{i,j} \equiv |\mathbf{r}_{i,j}|$. We assume periodic boundary condition. When the lattice is in the z-direction, the system Hamiltonian is given as

$$\mathcal{H} = -2J\sum_{j=1}^{N}((1+\alpha)(S_j^x S_{j-1}^x + S_j^y S_{j-1}^y) + (1-2\alpha)S_j^z S_{j-1}^z) - g\mu_B \sum_{j=0}^{N} \mathbf{S}_j \mathbf{H} \tag{2.34}$$

where

$$\alpha = -(g^2\mu_B^2/a^3)(1/2J), \tag{2.35}$$

$\mathbf{H}$ denotes the external magnetic field and $a \equiv |r_{i,j}|$. As we can see this equation, we can take into account the effect of the dipole-dipole interaction as an anisotropy effect.

They applied the Eq. (2.26) with the cases the external static magnetic field is parallel to z axis and also the case orthogonal to z axis. They used the Fisher's classical solution of spin-spin correlation function with zero magnetic field in classical vector type spin case, to calculate quantum spin-spin correlation function. They treated the effect of the external field as a perturbation to the zero field case. Then, they get the resonance shift from the paramagnetic case. We show the results in Fig. 5, which shows good agreement with the experiments.

2.8 Dzyaloshinsky-Moriya interaction

In considering the shape of the spin-spin interaction, the system may have the interaction as

$$\vec{d}[\mathbf{S}_i \times \mathbf{S}_j] \ . \tag{2.36}$$

This interaction is called as Dzyaloshinsky-Moriya interaction. Moriya performed the second order perturbation calculation between exchange interaction and orbital arguer momentum, and derived this term [25].

2.9 General theory of electron spin resonance

In this section, we review the general electron spin resonance theory start with Kubo formula.

We apply the weak oscillation field $\mathbf{H}e^{i\omega t}$. And we observe the magnetization $\mathbf{M}e^{i\omega t}$. Because the magnetic field is weak, so the following relation persists.

$$\mathbf{M} = \chi(\omega)\mathbf{H}. \tag{2.37}$$

$\chi(\omega)$ denotes the system susceptibility and in general, complex number. Here $\chi'(\omega)$ are real,

$$\chi(\omega) = \chi'(\omega) - i\chi''(\omega). \tag{2.38}$$

Here, $\chi''(\omega)$ stands for the energy absorption of the system. $\chi(\omega)$ and $\chi'(\omega)$ satisfy the Kramers Kronig relation. So with the measurement of $\chi''(\omega)$ in a wide range of ω, we can calculate $\chi'(\omega)$.

In electron spin resonance study, we observe the absorption of the energy applying the oscillating fields with various frequency. Below, we will derive $\chi''_{xx}(\omega)$ from Kubo formula. See appendix A for the derivation of Kubo formula.

Consider the case with no spontaneous magnetization. We apply the magnetic field $H^z(t')$ to the z axis direction and observe the response appears to the x axis direction. If we treat the response to M_x with the field H_z, the response function $\phi_{xx}(t-t')$ is defined as

$$\langle M^z(t)\rangle = \int_{-\infty}^{t} \phi_{xx}(t-t')H^z(t')\mathrm{d}t'. \tag{2.39}$$

In Kubo formula the response function is given as ,

$$\phi_{xx}(t-t') = i\langle[M^x(t), M^x(t')]\rangle, \tag{2.40}$$

where

$$\langle\cdots\rangle = \mathrm{Tr}\cdots \mathrm{e}^{-\beta\mathcal{H}}, \tag{2.41}$$

and β denotes

$$\beta = \frac{1}{k_{\mathrm{B}}T}, \tag{2.42}$$

with Boltzmann constant k_{B} and the temperature T. $\mathcal{H}$ is the system hamiltonian of the system. Here the pure quantum dynamics for time evolution is used.

$$M^x(t) = \mathrm{e}^{i\mathcal{H}t}M^x\mathrm{e}^{-i\mathcal{H}t}. \tag{2.43}$$

The response function is an odd function because the sign of the function changes when we exchanges t and t'. So, the left hand side of the Eq. (2.40) dose not change if we take complex conjugate. So, response function is real function.

We set the external magnetic field as

$$H^x(t') = \mathrm{Re}H_0\mathrm{e}^{i\omega t'}. \tag{2.44}$$

Here, Re denotes the real part.

Substituting the Eq. (2.44) to the Eq. (2.39) and set $t-t'$ as t', we obtain

$$\langle M^x(t)\rangle = \mathrm{Re}\int_0^{\infty} \phi_{xx}(t')\mathrm{e}^{-i\omega t'}\mathrm{d}tH_0\mathrm{e}^{i\omega t}, \tag{2.45}$$

because ϕ_{xx} is a real function. Here, the the complex susceptibility $\chi_{xx}(\omega)$ denotes as

$$\chi_{xx}(\omega) \equiv \int_0^{\infty} \phi_{xx}(t)\mathrm{e}^{-i\omega t}\mathrm{d}t \equiv \chi'_{xx}(\omega) - i\chi''_{xx}(\omega), \tag{2.46}$$

with real $\chi'_{xx}(\omega)$ and $\chi''_{xx}(\omega)$. As $\phi_{xx}(t)$ is the real odd function of t, we obtain as

$$\begin{aligned} -\mathrm{Im}\chi_{xx}(\omega) &= \chi''_{xx}(\omega) \\ &= \int_0^{\infty} \phi_{xx}(t)\sin\omega t\mathrm{d}t = \frac{1}{2}\int_{-\infty}^{\infty} \phi_{xx}(t)\sin\omega t\mathrm{d}t \\ &= -\frac{1}{2i}\int_{-\infty}^{\infty} \phi_{xx}(t)\mathrm{e}^{-i\omega t}\mathrm{d}t. \end{aligned} \tag{2.47}$$

Using the trace circulation,

$$\int_{-\infty}^{\infty}\langle M^x(t)M^x(0)\rangle \mathrm{e}^{-i\omega t}\mathrm{d}t = \int_{-\infty}^{\infty} Tr\mathrm{e}^{\beta\mathcal{H}}\mathrm{e}^{i\mathcal{H}t}M^x\mathrm{e}^{-i\mathcal{H}t}M^x\mathrm{e}^{i\omega t}\mathrm{d}t$$

$$= \int_{-\infty}^{\infty} Tr\mathrm{e}^{\beta\mathcal{H}}M^x\mathrm{e}^{i\mathcal{H}(t+i\beta)}M^x\mathrm{e}^{-i\mathcal{H}(t+i\beta)}\mathrm{e}^{-i\omega t}\mathrm{d}t. \tag{2.48}$$

Here, we set $t + i\beta$ as t.

$$= \mathrm{e}^{\beta\omega}\int_{-\infty}^{\infty}\langle M^x(0)M^x(t)\rangle \mathrm{e}^{-i\omega t}\mathrm{d}t \tag{2.49}$$

Substituting the Eq.(2.40) and the Eq.(2.49) for the Eq. (2.47) in order, we obtain the following expression.

$$\chi''_{xx}(\omega) = -\frac{1}{2}\int_{-\infty}^{\infty}\langle [M^x(t), M^x(0)]\rangle \mathrm{e}^{i\omega t}\mathrm{d}t = \frac{1}{2}(1-\mathrm{e}^{-\beta\omega})\int_{-\infty}^{\infty}\langle M^x(0)M^x(t)\rangle \mathrm{e}^{-i\omega t}\mathrm{d}t \tag{2.50}$$

In order to obtain $\chi''(\omega)$ practically, we proceed with the following procedures: First we obtain all the eigenvalues and the eigenvectors:

$$\mathcal{H}|m\rangle = E_m|m\rangle, \tag{2.51}$$

for $m = 1, \cdots M$. Here M is the total numbers of the states and $M = 2^N$ for $S = 1/2$ case. Here N is the number of spins. Next we obtain the matrix elements $\langle m|M^x|n\rangle$ for $m = 1, \cdots M$ and $n = 1, \cdots M$. With these quantities the autocorrelation function is given by

$$c(t) = \langle M^x(0)M^x(t)\rangle = \frac{\mathrm{Tr}M^x\mathrm{e}^{i\mathcal{H}t}M^x\mathrm{e}^{-i\mathcal{H}t-\beta\mathcal{H}}}{\mathrm{Tr}\mathrm{e}^{-\beta\mathcal{H}}}$$

$$= \frac{\sum_m\sum_n\langle m|M^x|n\rangle\mathrm{e}^{\mathrm{i}E_nt}\langle n|M^x|m\rangle\mathrm{e}^{-\mathrm{i}E_mt-\beta E_m}}{\sum_m\mathrm{e}^{-\beta E_m}}$$

$$= \frac{\sum_m\sum_n|\langle m|M^x|n\rangle|^2\mathrm{e}^{-\mathrm{i}(E_m-E_n)t}\mathrm{e}^{-\beta E_m}}{Z}. \tag{2.52}$$

where $Z = \sum_m \mathrm{e}^{-\beta E_m}$. The Fourier transformation of $c(t)$ is written as

$$\int_{-\infty}^{\infty} c(t')\mathrm{e}^{-\mathrm{i}\omega t'}\mathrm{d}t' = \frac{\sum_m\sum_n|\langle m|M^x|n\rangle|^2\mathrm{e}^{-\beta E_m}}{Z}2\pi\delta(\omega+(E_m-E_n)) \tag{2.53}$$

and $\chi''_{xx}(\omega)$ is given as an ensemble of the delta-functions:

$$\chi''_{xx}(\omega) = \sum_{\omega_{mn}} D(\omega_{mn})\delta(\omega+(E_m-E_n)), \tag{2.54}$$

where

$$D(\omega_{mn}) = \pi(1-\mathrm{e}^{-\beta\omega_{mn}})\frac{|\langle m|M^x|n\rangle|^2\mathrm{e}^{-\beta E_m}}{Z}$$

$$D(\omega_{mn}) = \pi(\mathrm{e}^{-\beta E_m}-\mathrm{e}^{-\beta E_n})\frac{|\langle m|M^x|n\rangle|^2}{Z} \tag{2.55}$$

and $\omega_{mn} = E_n - E_m$.

2.9.1 Perturbation expansion method

Natsume-Sasagawa-Toyoda-Yamada[20] calculated the shift of the resonance field when we change the angle between the chain and the fields with a perturbation calculation from Kubo formula. The system hamiltonian is one dimensional $S = 5/2$ Heisenberg model with exchange interaction, dipole-dipole interaction, and Zeeman term. This model is the relevant model corresponding to TMMC.

The absorption as $I(\omega)$ is given as

$$I(\omega) \propto \int_{-\infty}^{\infty} G(t) \mathrm{e}^{-i\omega t} \mathrm{d}t, \tag{2.56}$$

$$G(t) = \langle M^x(t) M^(0) \rangle. \tag{2.57}$$

Using the cumulant expansion of $G(t)$ toward the second order, They obtained as

$$\Delta H \propto -\sin^2\theta(3\cos 2\theta - 1)\cos 2\phi. \tag{2.58}$$

In Fig. 6 and Fig. 7, the geometrical configuration of the chain with θ and ϕ and the results are shown. They checked that their results agree with the experimental result of TMMC.

2.9.2 Theory with the dissipation term

Hamano *et.al* used the dynamics with dissipation term for $\mathbf{M}(t)$[21, 28]. Without dissipation effect, *i.e.* if we use pure quantum dynamics, the absorption function is described as assembly of delta functions, as Eq.(2.54). With the dissipation effect, each delta function will have a width.

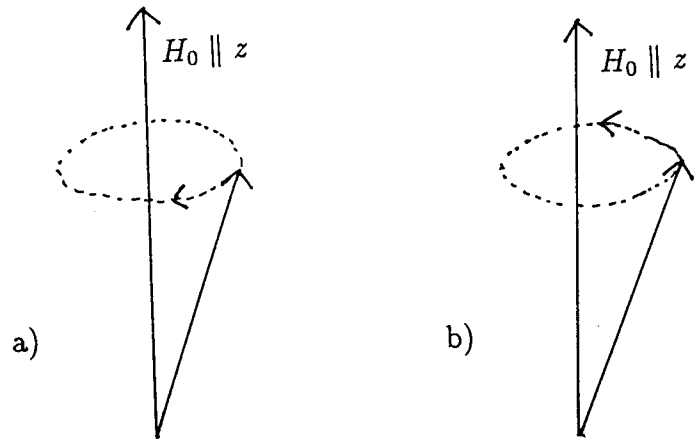

Fig. 4: The rough sketch of the Larmor rotation. (a) $\gamma > 0$ case , (b)$\gamma < 0$ case.

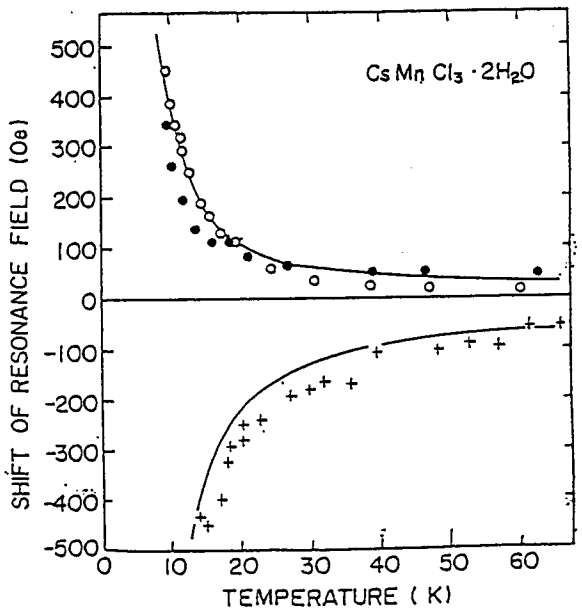

Fig. 5: The temperature dependence of the resonance shift, by Nagata-Tazuke, quotation from [7]. This experimental results of $CsMnCl_3 \cdot 2H_2O$ is also shown. The axes of the crystal are a, b and c. The chain is parallel to the a axis. •, , + in the figure are the experimental data, corresponding with the $H \parallel c$ case, the $H \parallel b$ case, and the $H \parallel a$ case. The Solid lines are theoretical results. Upper line denotes the case the chain and the static field H, and lower line denotes the case the chain is parallel to the static field. Corresponding data agrees well. The horizontal axis denotes the temperature (K), the vertical axes denotes the shift of the resonance field when we set the g value as 2.0.

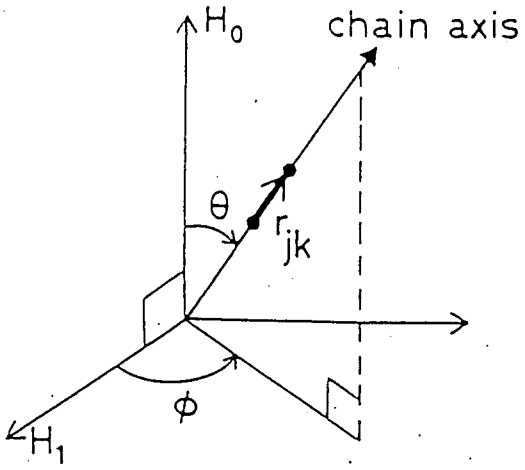

Fig. 1. Coordinate system of EPR for one-dimensional spin distribution. The microwave field H_1 is fixed to be perpendicular to the applied static field H_0 which is along the polar axis. The direction of chain axis is determined by both the polar (θ) and the aximuthal (ϕ) angles.

Fig. 6: The definition of ϕ and θ. Quotation form [20].

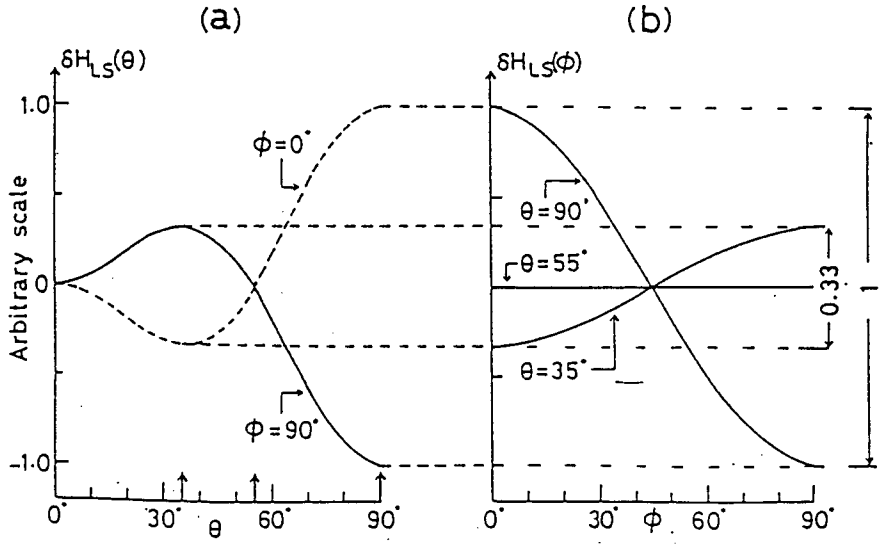

Fig. 2. Theoretical angular changes of the low-symmetric shift δH_{LS}. (a) The θ-dependences for the specific situations of ϕ=0° and 90°. (b) The ϕ-dependences at three characteristic angles of θ.

Fig. 7: ϕ and θ dependence of the resonance field. Quotation from [20].

Chapter 3

Method of Direct Numerical Analysis

3.1 Problems of the theories before

As described in the chapter 1 and 2, ESR in a low dimensional quantum spin system attracts interests both theoretically and experimentally. We focus on the ESR absorption line shape in such a system.

Nagata and Tazuke have used the Kanamori-Tachiki formula to obtain the temperature dependence of the resonance of the one dimensional Heisenberg antiferromagnet with the dipole interaction. They succeeded in explaining experimental data of the shift in $CsMnCl_3 \cdot 2H_2O$.[7] This approach is a seminal step to investigate the ESR measurement from a microscopic viewpoint. Their method, however, aimed at studying collective motion of spins in ordered systems and assumed only one dominant mode. Furthermore, for the practical calculation, informations of the spin system at finite temperatures, such as the temperature dependence of the spin correlation function, etc. are necessary, which should be provided from other studies.

Generally in the quantum disorder states, the spin correlation function decays in a short distance. Thus it is expected that we can obtain characteristic features of ESR line shape by studying the response function of a finite spin cluster of the system including the dipole interaction. The system may have Dzyaloshinsky-Moriya interaction.

under this circumstance we propose a direct numerical approach to this problem. Here we study the response function given by the Kubo formula[8, 9, 39] in a way of the first principle although we limit the size of the system to rather small number. Here we use non-approximated quantum mechanical dynamics of spins due to the exchange interaction and the dipole interaction.

3.2 The elementary procedure

We starts from Eq.(2.54) and Eq. (2.55). We show them again below as

$$\chi''_{xx}(\omega) = \sum_{\omega_{mn}} D(\omega_{mn})\delta(\omega + (E_m - E_n)), \tag{3.1}$$

$$D(\omega_{mn}) = \pi(\mathrm{e}^{-\beta E_m} - \mathrm{e}^{-\beta E_n})\frac{|\langle m|M^x|n\rangle|^2}{Z}. \tag{3.2}$$

(ω_{mn} is denoted as $\omega_{mn} = E_n - E_m$.)

We should note that we should do diagonalization of the complex Hermitian matrix, generally.

For absorption, we consider the case with $\omega_{mn} > 0$. Because we do not include the dissipation effect, the susceptibility is an ensemble of the delta functions. Z is denoted by $Z = \sum_m \mathrm{e}^{-\beta E_m}$. When we need the broadening of each resonance we should use dynamics with dissipation effect as have been done by Hamano *et al.*[21, 28], (see section 2.9.2).

However, since we take into account the dipole and exchange interactions explicitly in $\mathcal{H}$, we can treat the broadening due to them in the way of the first principle.

We study the temperature dependence of the mean of the frequency and its width by

$$\bar{\omega} = \frac{\sum_{\omega_{mn}} \omega_{mn} D(\omega_{mn})}{\sum_{\omega_{mn}} D(\omega_{mn})}, \tag{3.3}$$

and

$$\Delta\omega = \sqrt{\frac{\sum_{\omega_{mn}} \omega_{mn}^2 D(\omega_{mn})}{\sum_{\omega_{mn}} D(\omega_{mn})} - \bar{\omega}^2}, \tag{3.4}$$

respectively.

After here, we translate the resonance frequency $\bar{\omega}$ to a δH, the shift of the resonance field from the paramagnetic resonance field.

In the isotropic Heisenberg model case, where no anisotropy effect of interaction, the relation between the resonance field H_{R} and the resonance field ω_{R} are shown as

$$\omega_{\mathrm{RO}} = \gamma H_{\mathrm{RO}}. \tag{3.5}$$

This relation is identical with paramagnetic resonance case. Here, the gyromagnetic rate γ is denoted as $\gamma = \frac{1}{2} g_{\mathrm{e}} \mu_B / \hbar$.

We need the term which breaks SU(2) symmetry if we want to see the resonance shift from the paramagnetic case. The dipole-dipole interaction term is one of the such a term. In experiments, we fix the detecting field angular frequency ω_{RO} and change the strength of the static magnetic field H_0, investigating the peak of the absorption. Assume that when

$$H_0 \to H_0 + \Delta H,$$

the absorption amplitude becomes local maximum, i.e. resonance peak has detected. We can describe this change that g value shifts with H_0 is fixed, as

$$\omega = \frac{g'\mu_{\rm B}(H_0 + \Delta H)}{\hbar} \tag{3.6}$$

$$g \to g \times \frac{H_0}{H_0 + \Delta H} \simeq g - g\frac{\Delta H}{H_0}. \tag{3.7}$$

The minus change of δH_0 corresponds to the positive change of $g_{\rm eff}$.

In actual numerical calculation, we fix H_0 and change ω, detecting the absorption peak, first. The resonance angular frequency shift from the paramagnetic resonance angular frequency ω_{RO}, $\Delta\omega$, is given as

$$\Delta\omega = \omega - \omega_{\rm RO}. \tag{3.8}$$

Here, the shift of the resonance field is given as

$$\Delta H = \frac{1}{\gamma}(\omega + \Delta\omega) - H_0. \tag{3.9}$$

Note that γ becomes 1.0 if we set $\frac{\mu_B}{\hbar} = 1$, because $g_{\rm e} = 2.0$.

In order to obtain the line shape we construct a histogram representing $\chi''(\omega)$ with a small interval $\delta\omega$. In the k-th bin, we sum up $D(\omega_{mn})$ over ω_{mn} in the interval $k\delta\omega \sim (k+1)\delta\omega$. Even for small number of N, the total number of states M is large, and furthermore the number of frequencies $\{\omega_{mn}\}$ is $O(M^2)$. Thus we obtain a rather smooth line shape.

3.3 Hamiltonian with the dipole interaction

The hamiltonian of the system with the static field H_0 is given by

$$\mathcal{H} = \mathcal{H}_0 + \mathcal{H}_{\rm D} - \mathbf{H}_0 \cdot \mathbf{M}, \tag{3.10}$$

where $\mathcal{H}_0$ is the spin hamiltonian of the system denoted by

$$\mathcal{H}_0 = \sum_i^N (2J_i \mathbf{S}_i \mathbf{S}_{i+1}). \tag{3.11}$$

N is the system size and take periodic boundary condition, i.e. ,$S_{N+1} = S_1$. $\mathcal{H}_{\rm D}$ denotes the dipole interaction:

$$\mathcal{H}_{\rm D} = D\sum_{ij}\left(\frac{\mathbf{S}_i \cdot \mathbf{S}_j}{r_{ij}^3} - \frac{3(\mathbf{S}_i \cdot \mathbf{r}_{ij})(\mathbf{S}_j \cdot \mathbf{r}_{ij})}{r_{ij}^5}\right), \tag{3.12}$$

where $\mathbf{r}_{ij}$ is the vector from the site i to j and $r_{ij} = |\mathbf{r}_{ij}|$. Let the direction of $\mathbf{r}_{ij}$ be (α, β, γ), ($\alpha = \cos\phi_{ij}\sin\theta_{ij}, \beta = \sin\phi_{ij}\sin\theta_{ij}$ and $\gamma = \cos\theta_{ij}$). Here $\mathbf{M}$ $(= \sum_i \mathbf{S}_i)$ is the total magnetization and $\mathbf{H}_0$ represents the external static field in the direction (θ_H, ϕ_H) with an amplitude $H_0 = |\mathbf{H}_0|$. In Fig. 8, the geometry of $\mathbf{H}_0$ and $\mathbf{r}_{ij}$ is given.

First we write down the hamiltonian $\mathcal{H}_0+\mathcal{H}_D$ which consists of the exchange interactions. Generally the interaction between two spins is given by

$$\mathcal{H} = (S^x, S^y, S^z) \begin{pmatrix} h_{11} & h_{12} & h_{13} \\ h_{21} & h_{22} & h_{23} \\ h_{31} & h_{32} & h_{33} \end{pmatrix} \begin{pmatrix} S^x \\ S^y \\ S^z \end{pmatrix}, \tag{3.13}$$

where

$$\begin{aligned} h_{11} &= -2(J_x + D_0(\alpha^2 - \tfrac{1}{3})) \\ h_{22} &= -2(J_y + D_0(\beta^2 - \tfrac{1}{3})) \\ h_{33} &= -2(J_z + D_0(\gamma^2 - \tfrac{1}{3})) \\ h_{12} &= -2D_0\alpha\beta \\ h_{23} &= -2D_0\beta\gamma \\ h_{31} &= -2D_0\gamma\alpha \end{aligned} \tag{3.14}$$

where $D_0 = 3D/2r_{ij}^3$.

We show the explicit expression of H_{ij} in Pauli Matrix when $S = 1/2$ in Appendix B.

In practical calculations, we take the direction of the field as the diagonalization axis. Thus we rotate the axis using the matrix:

$$R = \begin{pmatrix} \cos\theta_H \cos\phi_H & \cos\theta_H \sin\phi_H & -\sin\theta_H \\ -\sin\phi_H & \cos\phi_H & 0 \\ \sin\theta_H \cos\phi_H & \sin\theta_H \sin\phi_H & \cos\theta_H \end{pmatrix}. \tag{3.15}$$

In the new axis the interaction $\mathcal{H}_{ij}$ is given by

$$\tilde{\mathcal{H}} = R\mathcal{H}\,{}^tR. \tag{3.16}$$

Now we diagonalize an $M \times M$ Hermitian matrix $\tilde{\mathcal{H}} - H_0M_z$, where $M_z = \sum_i S_i^z$ is the z component of the magnetization in the new coordinate. Generally speaking, this matrix is complex Hermitian matrix. We apply a detecting field along the x or y axis in the new coordinate, *i.e.* $-H_1\cos(\omega t)\sum_i S_i^x$ for $\chi''_{xx}(\omega)$, and $-H_1\cos(\omega t)\sum_i S_i^y$ for $\chi''_{yy}(\omega)$. Using the eigenvalues and eigenvectors, $\{E_m\}$ and $\{|m\rangle\}$ $(m = 1, \cdots M)$, we obtain the line shape (2.54).

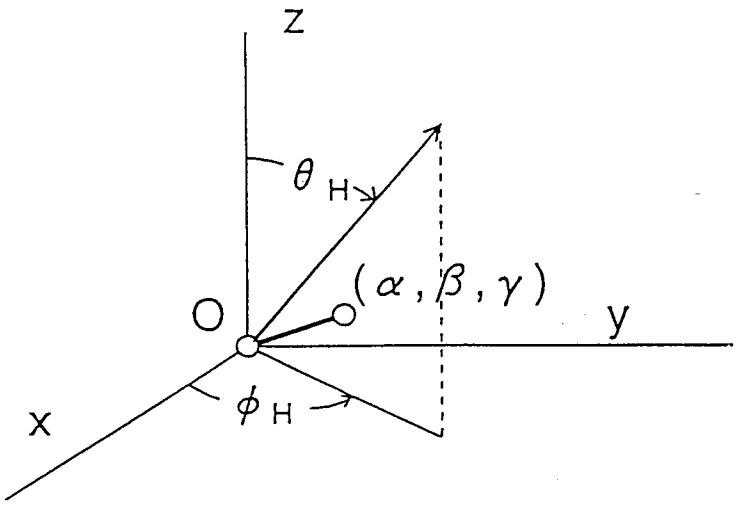

Fig. 8: One dimensional spin chain and the static field.

Chapter 4

Antiferromagnetic Heisenberg chain

We apply our method to the one dimensional Heisenberg model in various geometrical configurations of the lattice and the external fields, *i.e.* the static field and the detecting oscillating field. We investigate how the resonating frequency shifts due to the dipole interaction and anisotropy of the interaction. We confirm that the present method reproduces qualitative features of the results of Nagata and Tazuke for the dependence of the shift on the angle between the lattice and the static field. We also investigate the angle dependence of the width and obtain a good agreement with the experimental data of Dietz *et al.*[36, 37] The shift also depends on the angle between the lattice and the oscillating field.[20] We find that the temperature dependence is sensitive to the strength of the static field. At weak fields, we find a dependence which qualitatively agrees with a recent experimental study of TMMC by Taniguchi *et al.* [29]

We use $\mathbf{H}_0$ to express the static field, and use $\mathbf{H}_1$ to express the oscillating field.

We assume the static magnetic field is orthogonal to the oscillating field. Thus as the most typical cases of geometrical configurations of the lattice, the static field and oscillating filed, there are six configurations. (Fig. 9) There, H_0 denotes the static magnetic field, and H_1 denotes the oscillating field. Hereafter we call the cases following in Fig. 9.

In this chapter we apply the present method to the one dimensional antiferromagnetic Heisenberg model:

$$\mathcal{H}_0 = 2J \sum_{i=1}^{L} \mathbf{S}_i \cdot \mathbf{S}_{i+1} \tag{4.1}$$

with the periodic boundary condition $\mathbf{S}_{L+1} = \mathbf{S}_1$. Hereafter we use $J(> 0)$ as a unit of energy. Here we take the value of D for the dipole interaction (3.12) to be $3D/a^3 = (2/27)J$ with $a = r_{ij}$, $(D_0 = J/3^3)$.

First let us study the case where the direction of the chain is perpendicular to the field $\mathbf{H}_0$. That is to say, $(\alpha, \beta, \gamma) = (1, 0, 0)$ and $\theta_H = 0$ and $\phi_H = 0$, which will be called the Case1. In Fig. 10, a typical histogram representing $\chi''_{xx}(\omega)$ is shown. In Fig. 11, that for $\theta_H = \pi/2$ and $\phi_H = 0$ is given, where the chain and $\mathbf{H}_0$ are parallel, which will be called the Case3.

In Fig. 12, the temperature dependence of the shift ΔH, eq.(3.9), is shown for various values of θ_H. We find that δH is positive in the Case1, while it is negative in the Case3. The amplitudes of the shifts increase at low temperatures. These qualitative features agree with the results of Nagata-Tazuke. Although we do not show here, for small values of H_0, it is also found that values of the shifts $\Delta H(T)$ move downwards and $\Delta H(T)$ is negative for most angles, and that amplitude of these shifts becomes large as H_0 becomes small, which is naturally expected.

In Fig. 13, we show the dependence of ΔH on the angle θ_H keeping $\phi_H = 0$. We find that the shift disappears around $\theta_H = \pi/6$. This is the angle which has been known as the magic angle, $3\cos^2(\pi/2 - \theta) - 1 = 0$, where the anisotropy due to the dipole interaction disappears.[36, 37]

In ESR theory of a single spin (EPR) [8, 9, 39], the line shape has been studied in terms of the nature of random noise. In the present analysis, we can directly obtain the line shape due to the exchange interaction and the dipole interaction. The data of the width $\Delta\omega$ are shown in Fig. 14 which agree qualitatively well with the experimental data for TMMC.[36, 37]

Effects of long time diffusive behavior of the random force has been also discussed in order to study the type of the line shape.[36, 37] Such slow random noise comes from the collective motion of the spin due to the exchange energy. In the present analysis, the spin dynamics due to the exchange interaction is taken into account and thus effects of such interactions are included automatically. However as shown in Figs. 10 and 11, it is difficult to discuss the type of the shape whether Lorentzian, Gaussian or other type. Because the system studied here is not large, the effects due to the slow collective mode does not appear here. Thus we simply estimated the width by Eq.(3.4) which corresponds to the width of Gaussian shape. We restrict the summation in Eq.(3.4) near the peak because $D(\omega_{mn})$s for large $\omega_{mn} - \bar{\omega}$ cause significant effects on the summation for the width even if $D(\omega_{mn})$s themselves are very small. For the data in Figs. 12 , 13 and 14, we take the summations in the range $0.9H_0 \leq \omega \leq 1.1H_0$, which seems reasonable from the observation in Figs. 10 and 11.

Next we investigate the shift in the configurations between the Case1 and the Case2 where $(\alpha, \beta, \gamma) = (0, 1, 0)$ and $\theta_H = 0$. Here the static field is always perpendicular to the lattice. On the other hand, the angle ϕ_{ij} between the lattice and the detecting field changes from 0 (Case1) to $\pi/2$ (Case2). Generally $\chi''_{xx}(\omega)$ depends on the angle ϕ_{ij} because of the difference of geometrical configurations. This dependence is called dynamical shifts.[20, 29]

In Figs. 15 and 16, the shifts are plotted for various values of angle ϕ_{ij}. For a strong field, *i.e.* $H_0 = 1.0$, we find very weak dynamical shift. That is to say, the shifts are almost the same regardless to the angle ϕ_{ij}. Here the shift in $\chi''_{yy}(\omega)$ and $\chi''_{xx}(\omega)$ are nearly the same.

On the other hand, for a weak field, ϕ-dependence of the shifts becomes significant. In particular, for $H_0 = 0.3$, we find that the temperature dependence of the shift in the

Case1 is in opposite direction to that in the Case2. This dependence has been observed by Taniguchi *et al.* in TMMC[29]. Here it should be noted that Taniguchi *et al.* have found very symmetric shifts, *i.e.* ΔH in the Case1 $\simeq -\Delta H$ in the Case2, while here we found an asymmetric one. In the present model, the $\cos 2\phi$ type dependence[20] is found at high temperatures, but $\chi''_{xx}(\omega)$ in the Case2 depends on H_0 strongly at low temperatures as shown in Fig. 17. Furthermore the width of the shape is rather wide when the dynamical shift is notable. In Fig. 18 the line shape for $H_0 = 0.3$ at a high temperature is shown. We find that the line shape decomposes to several peaks at low temperatures. (Fig. 19) These detailed properties may depend on the value of the spin, *i.e.*

Because of the geometrical equivalence, there are some trivial properties, *i.e.* the shift must not depend on θ_H in the Case2, and $\chi''_{yy}(\omega)$ in the Case1 is the same as $\chi''_{xx}(\omega)$ in the Case2. These properties have been confirmed to check the reliability of the present method. In this paper we studied mainly the chain with $N = 8$. We have checked that the qualitative features do not change for $N = 6$ and $N = 10$.

Next we also study the effect of the edge. Because spins at edges behave more freely and may affect on the response. In Fig. 20 the shifts are shown for the periodic chain (solid line) and for the open chain (dashed line) in the configuration of the Case1. We find the shift is almost the same but the shift in the open chain is smaller at low temperatures. This observation seems natural because the system in an open chain is close to the free spin for which no shift appears.

4.1 Effects of anisotropy

Besides the dipole interaction, the system may have an anisotropic coupling:

$$\mathcal{H}_0 = 2J \sum_{i=1}^{L} (S_i^x S_{i+1}^x + S_i^y S_{i+1}^y + A S_i^z S_{i+1}^z). \tag{4.2}$$

In Fig. 21, the shift in the configuration of the Case1 for the XY anisotropy ($A = 0.9$) is plotted. We find that shifts become large and remain nonzero even at high temperatures. Here it should be noted that the dependence of the shift on the angle θ_H is opposite to that in Fig. 12. We found that the shift is very sensitive to the anisotropy and the dependence changes around $A = 0.96$ where the shifts for all values of ϕ almost coincide, where the anisotropy is effectively compensated by the dipole interaction.

Next we study the case of Ising anisotropy. The θ_H dependence of the shift is similar to that for the Heisenberg model (Fig. 12). When the anisotropy increases, however, the dependence of the shift on the temperature and the angle shows various features. For example, in the case of $A = 1.2$, for a weak field $H_0 = 0.3$ the shifts for all the θ_H appear in the negative side as shown in Fig. 22, while for a strong field $H = 1.0$ the θ_H dependence of the shift changes qualitatively with the temperature as shown in Fig. 23.

While the anisotropy is only effectively compensated by the dipole interaction in the Case1, the anisotropy is canceled exactly in the Case3 where the lattice and the static field are parallel. This cancelation occurs when $H_{11} = H_{22}$ coincides with H_{33} in Eq.(3.14), *i.e.* $J_x = J_y = J_z + D_0$, which corresponds to $A = 1 + D_0 \simeq 1.037$. At this anisotropy, we have checked that $\Delta H = 0$.

4.2 Antiferromagnetic Heisenberg Chain,Summary and Discussion

We have investigated shifts of the resonance peak of ESR for antiferromagnetic Heisenberg chains in various geometrical configurations and also the anisotropy effects on the shifts. In particular, we investigated the dependence of the shift ΔH on the angle θ_H, which agrees with the results of Nagata and Tazuke. [7] We also investigated the width of the resonance $\Delta\omega$ due to the dipole interaction and the exchange interaction. The angle dependence of the width also agrees with the corresponding experiments. [36, 37] The field- and temperature-dependence of the dynamical shift was also investigated and found a case corresponding the experiments by Taniguchi *et al.* [29] So far we compared our data with those of TMMC($S = 5/2$) but it would be very interesting to compare them with data of an $S = 1/2$ antiferromagnetic Heisenberg chain.

Here let us mention for the shift in the ferromagnetic chain. The angle dependence of the shift in the configuration of Fig. 12 has been found very similar to that of the antiferromagnetic chain. The dynamical shift also shows similar behavior at high temperatures. On the other hand, at low temperatures the dynamical shift increases (move upwards) regardless to the angle ϕ_{ij}.

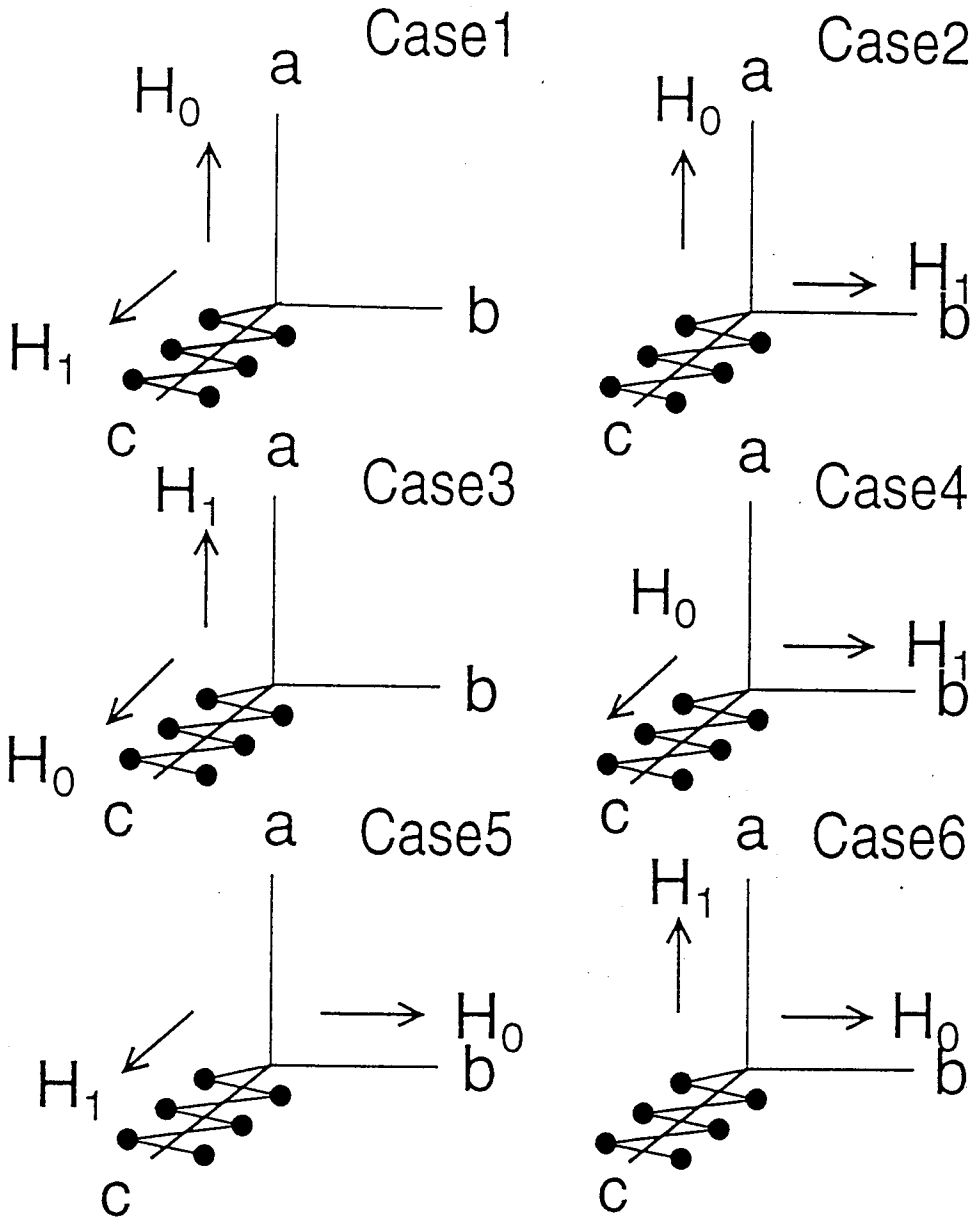

Fig. 9: Geometrical Six Configurations with $\mathbf{H_0}$,$\mathbf{H_1}$,and chain direction.

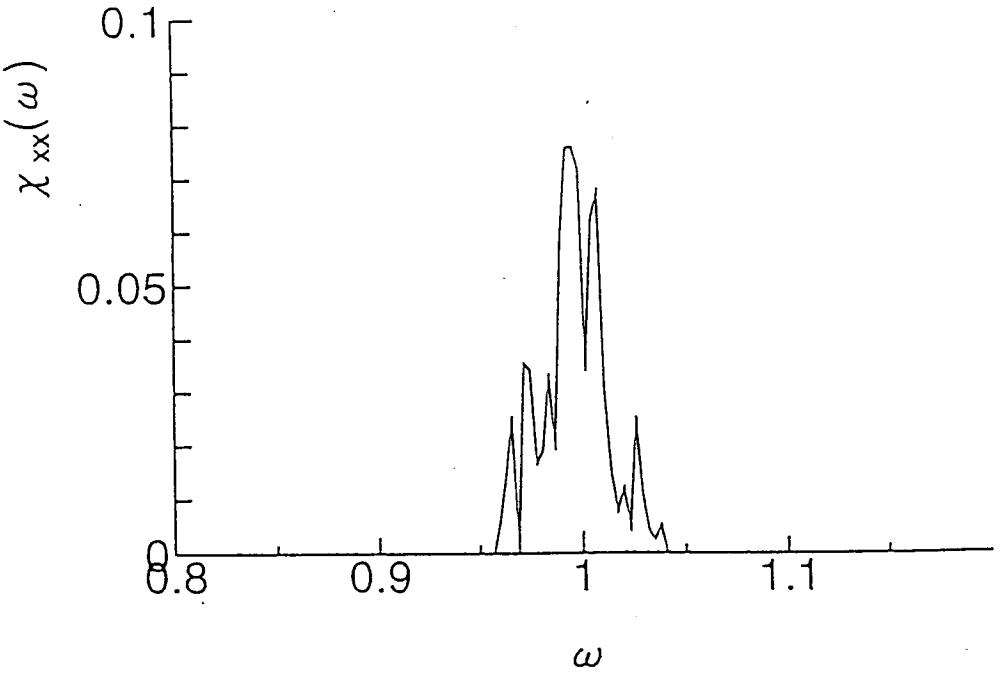

Fig. 10: $\chi_{xx}(\omega)$ as a function of the frequency ω for $H_0 = 1.0$ at $T = 4.0$. in the configuration of the Case1.

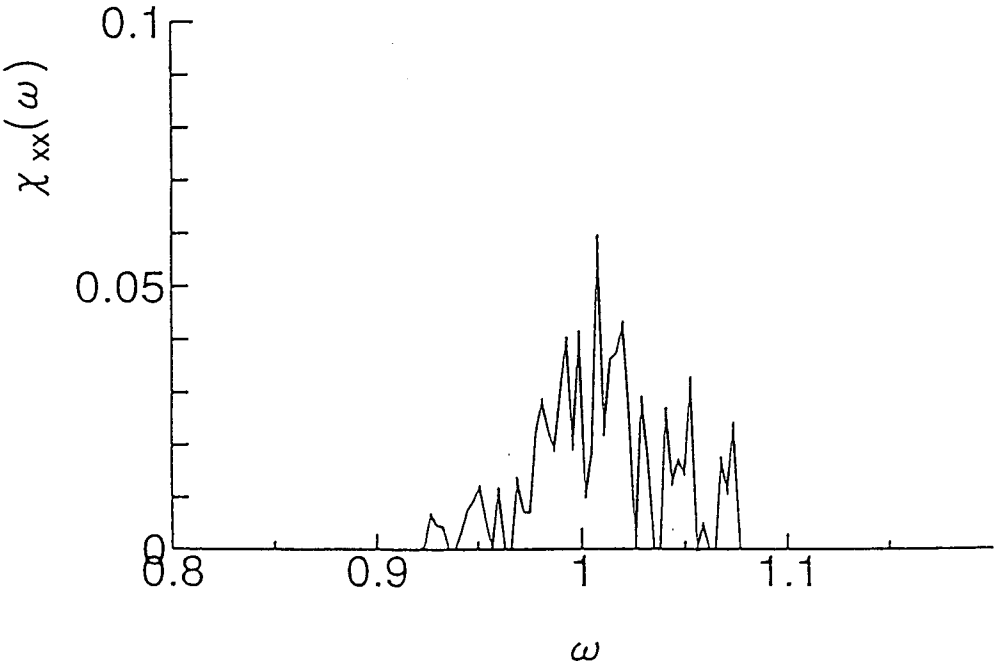

Fig. 11: $\chi_{xx}(\omega)$ as a function of the frequency ω for $H_0 = 1.0$ at $T = 4.0$. in the configuration of the Case3.

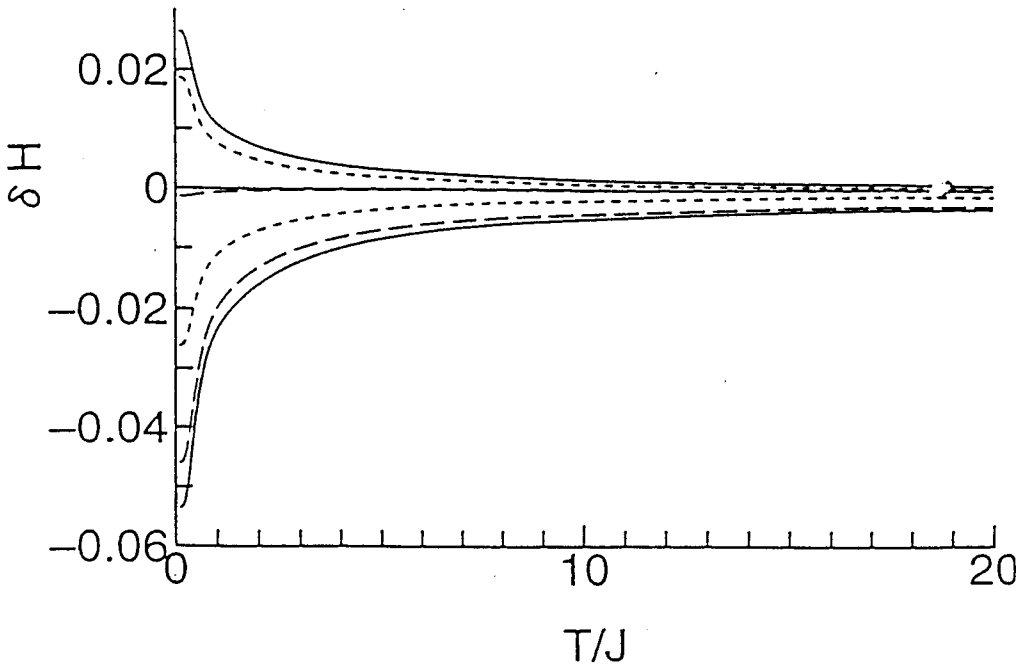

Fig. 12: The shift of resonance, $\delta H(T)$ for $H_0 = 1.0$ in configurations of $\theta_H = m \times \pi/10$, m=0,1,2,3,4, and 5 (from the top to the bottom), which changes the configuration from the Case1 to Case3.

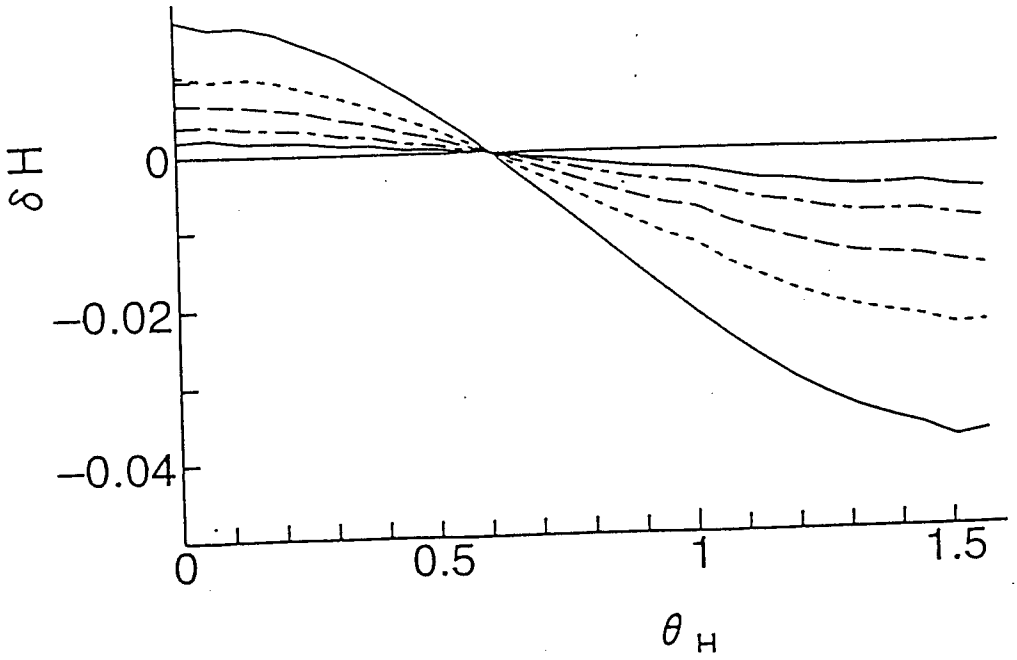

Fig. 13: The angle θ_H dependence of the data in Fig. 12 for the temperatures, $T = 0.5, 1.0, 2.0, 4.0$ and 8.0 from the top to the bottom at $\theta_H = 0$.

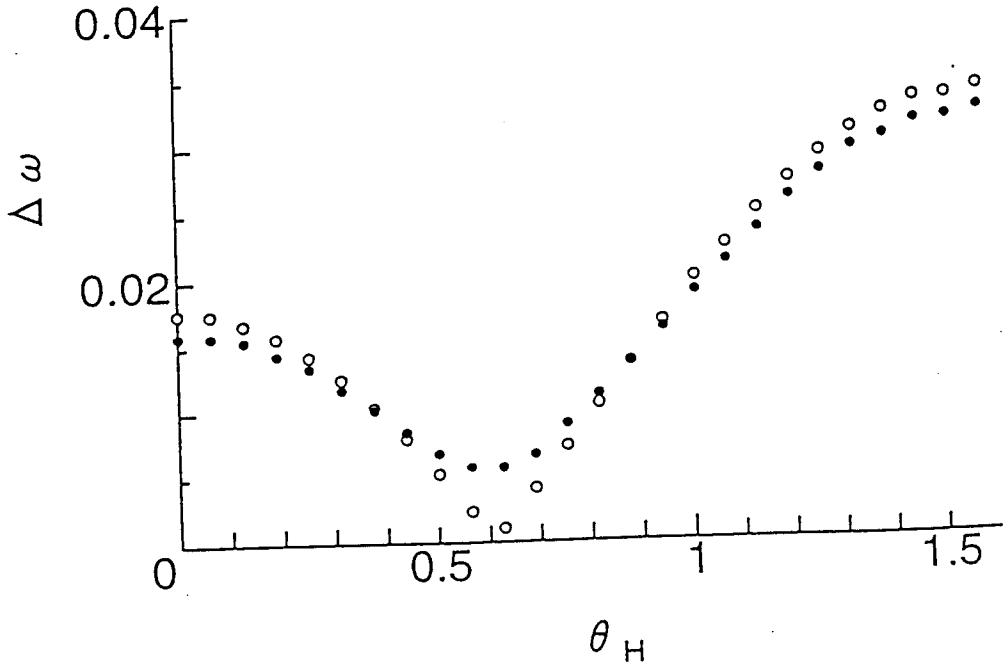

Fig. 14: The angle dependence of the width $\Delta\omega$: open circles denote the data for $T = 0.5$ and the closed circles $T = 8.0$.

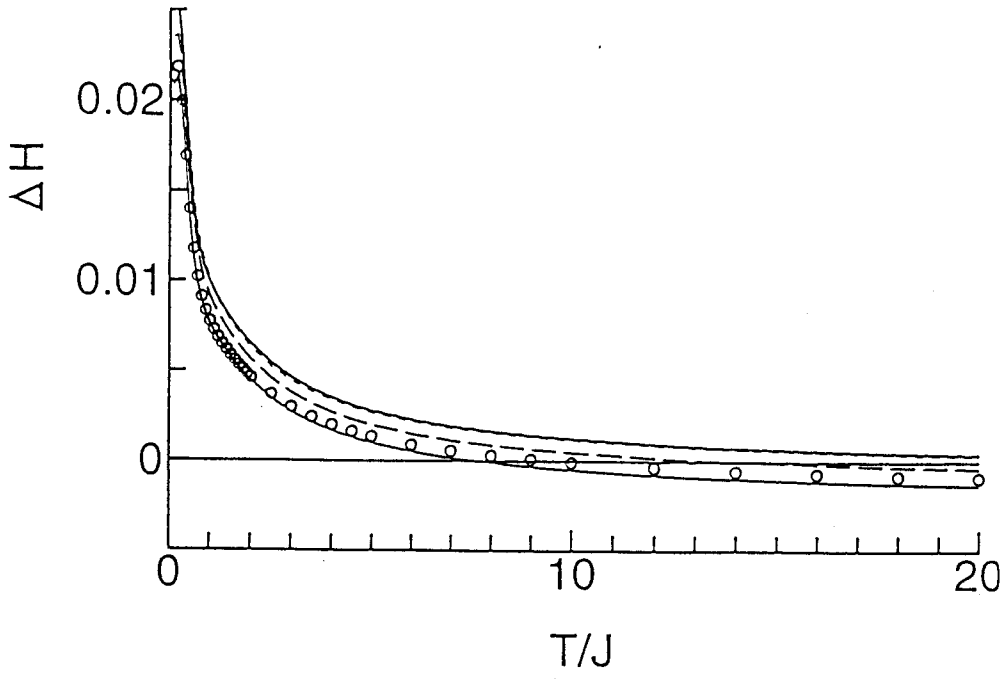

Fig. 15: The shift of resonance, $\delta H(T)$ for $H_0 = 1.0$ in configurations from the Case1 to Case3. The lines denote data for $\phi_{ij} = 0, \pi/10, \pi/4$, and $\pi/2$ from the top to the bottom. The circles denote data for $\phi_{ij} = 2\pi/5$.

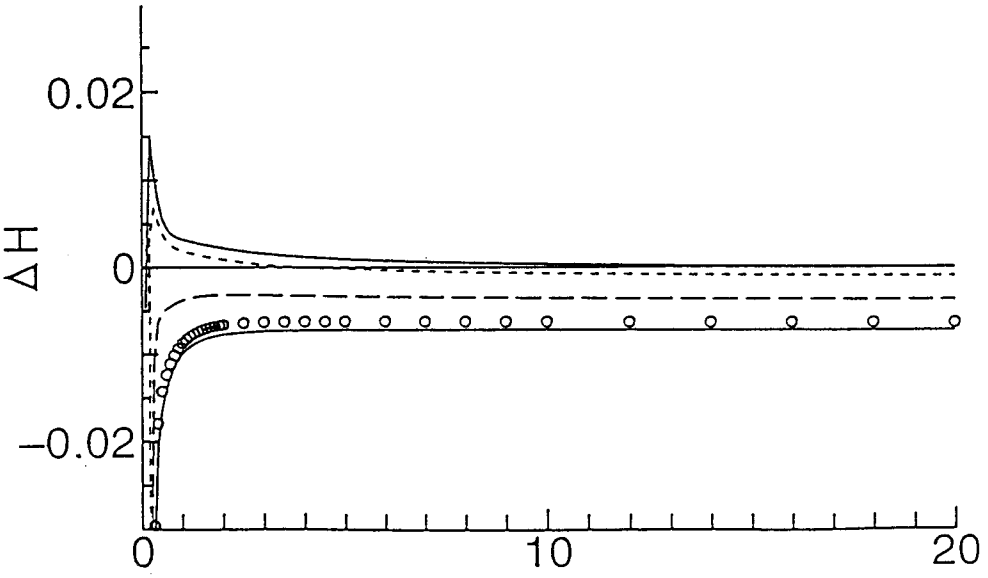

Fig. 16: The shift of resonance, $\delta H(T)$ for $H_0 = 0.3$ in configurations from the Case1 to Case3. The lines denote data for $\phi_{ij} = 0, \pi/10, \pi/4$, and $\pi/2$ from the top to the bottom. The circles denote data for $\phi_{ij} = 2\pi/5$.

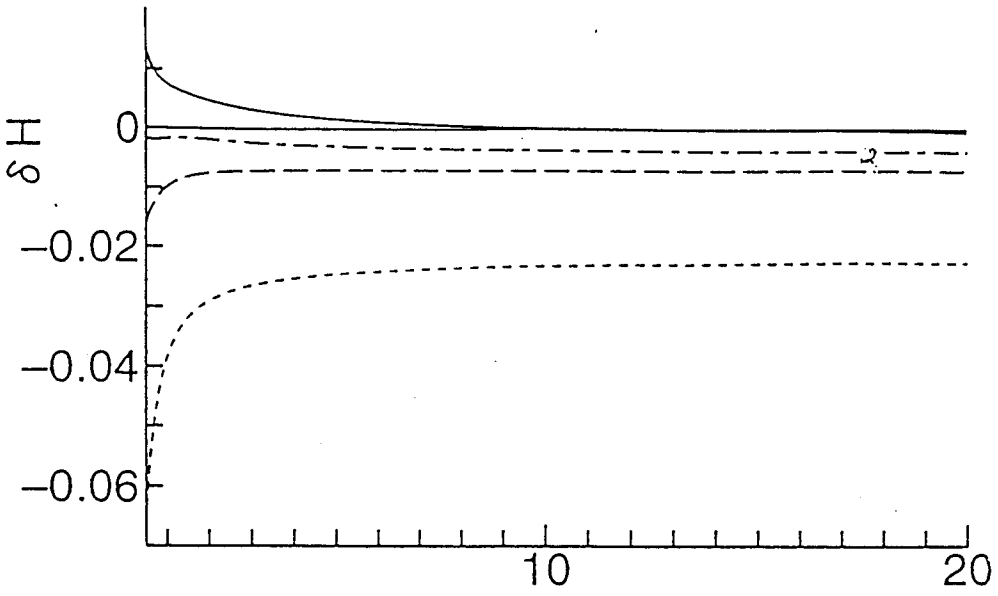

Fig. 17: H_0 dependence of the shifts for $\phi_{ij} = \pi/2$. Lines correspond to data for $H_0 = 1.0, 0.5, 0.3$ and 0.1 from the top to the bottom.

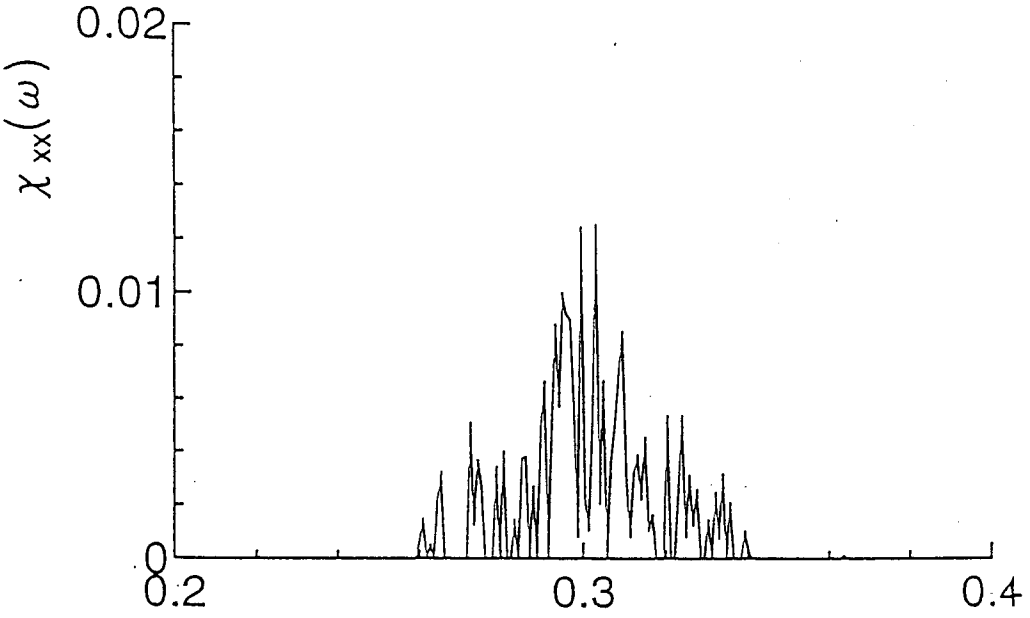

Fig. 18: Line shapes of the data in Fig. 17 with $H_0 = 0.3$, $T = 4.0$.

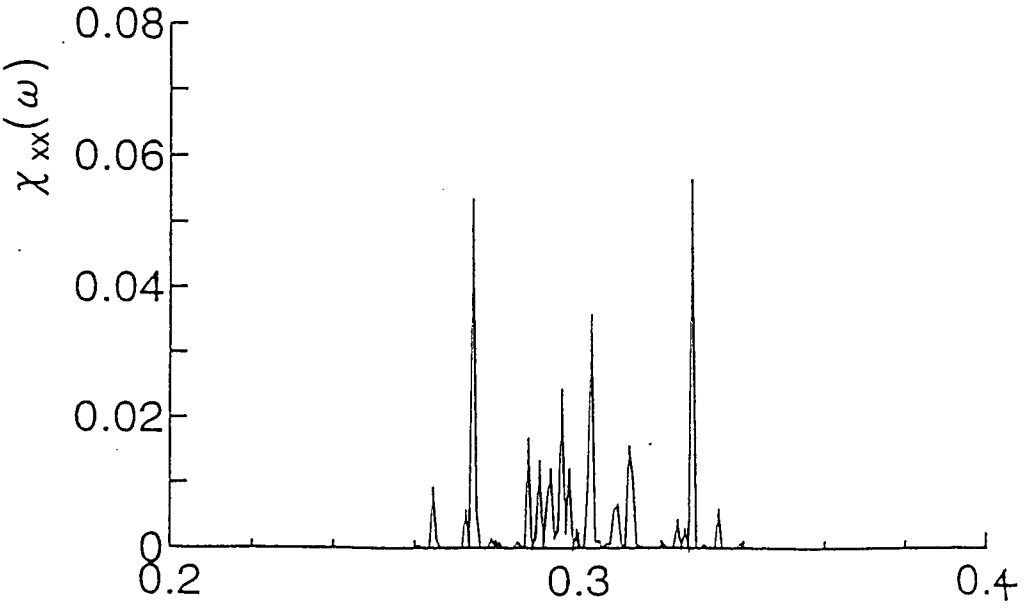

Fig. 19: Line shapes of the data in Fig. 17 with $H_0 = 0.3$, $T = 1.0$.

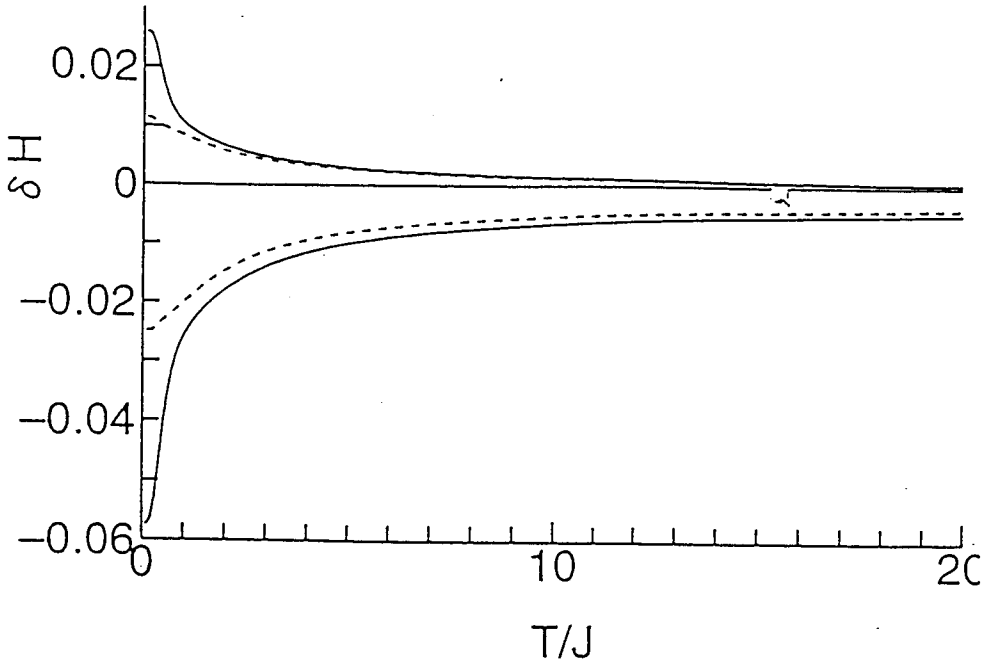

Fig. 20: Dependence of the boundary conditions in the same configurations for Fig. 12 (only for $\theta_H = 0$ and $\pi/2$): the solid lines denote the dependence in the periodic boundary condition and the dashed line in the open chain.

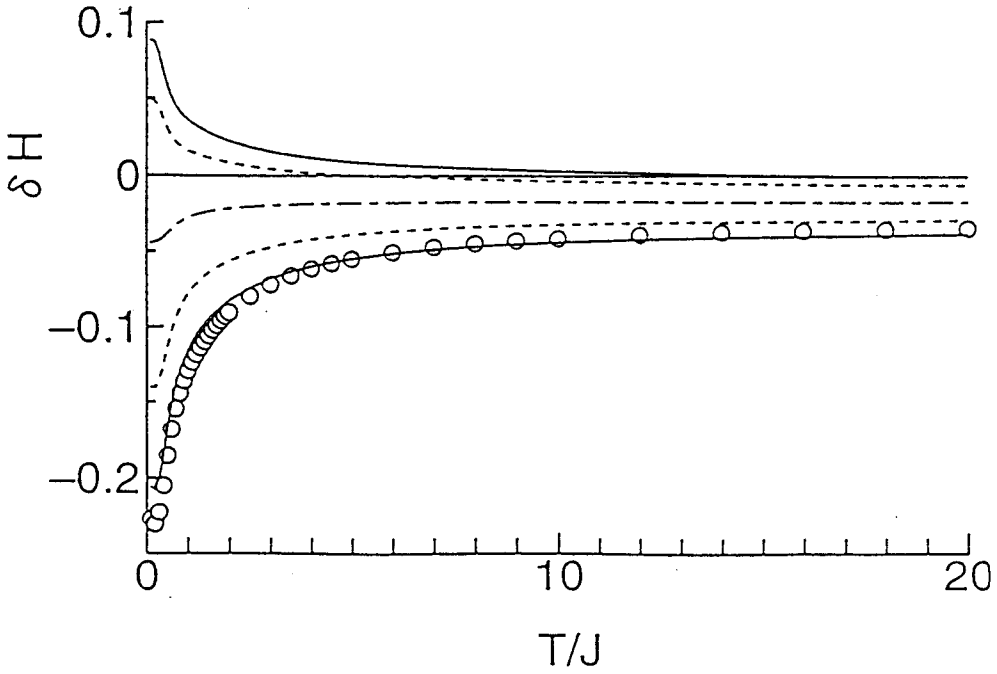

Fig. 21: The shift of resonance, $\delta H(T)$ for $H_0 = 1.0$ in the same configurations for Fig. 12 for XY anisotropic interaction ($H_0 = 1.0$ and $A = 0.9$). The circle denotes the data for $\theta_H = 0$ and the lines denote data for $\theta_H = m\pi/10$, $m = 1, 2, 3, 4$ and 5 from the bottom to the top.

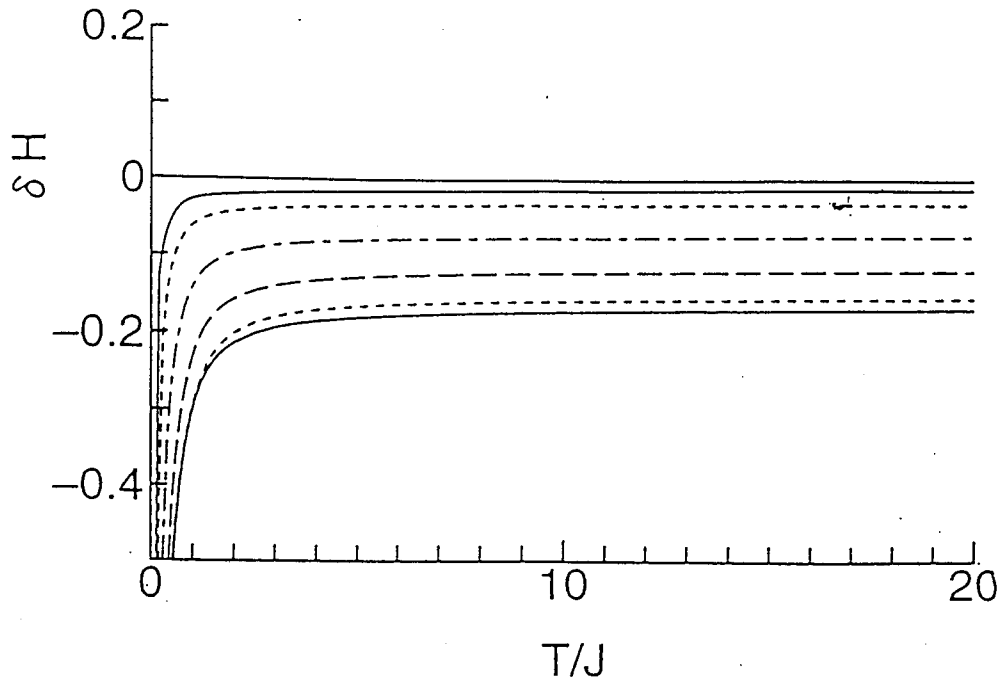

Fig. 22: The shift of resonance, $\delta H(T)$ in the same configurations for Fig. 12 for Ising anisotropic interaction ($H_0 = 0.3$ and $A = 1.2$). $\theta_H = 0, \pi/10, \pi/5, 3\pi/10, 2\pi/5$ and $\pi/2$ from the top to the bottom at $T = 20$.

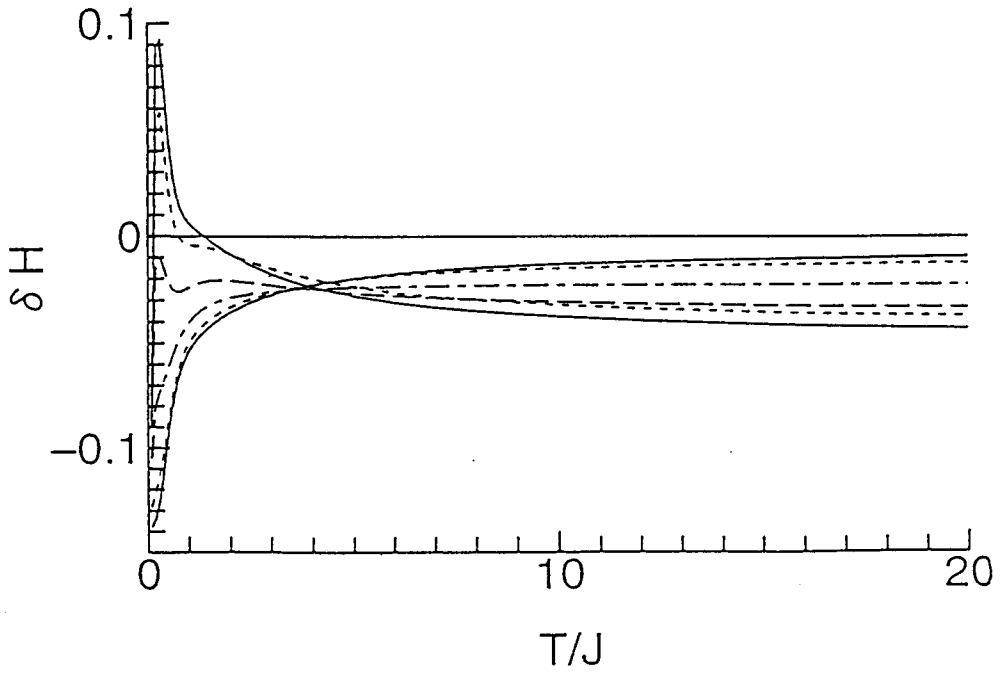

Fig. 23: The shift of resonance, $\delta H(T)$ in the same configurations for Fig. 12 for Ising anisotropic interaction ($H_0 = 1.0$ and $A = 1.2$). $\theta_H = 0, \pi/10, \pi/5, 3\pi/10, 2\pi/5$ and $\pi/2$ from the top to the bottom at $T = 20$.

Chapter 5

ESR in Zigzag Chain

The relevant model to the material $Cu_{0.9}Zn_{0.1}Nb_2O_6$ is a one dimensional $S = 1/2$ chain with zigzag structure. We study the electron spin resonance of this model.

5.1 The geometrical constants of $Cu_{0.9}Zn_{0.1}Nb_2O_6$ and the system hamiltonian

Motivated by the experiments on $Cu_{0.9}Zn_{0.1}Nb_2O_6$ we investigate a chain with zigzag structure. $Cu_{0.9}Zn_{0.1}Nb_2O_6$ has a quasi one dimensional lattice with a zigzag chain of $S = 1/2$ spins of Cu which are coupled by ferromagnetic and antiferromagnetic bonds alternately. The zigzag chain has tree principal axes $(\vec{a}, \vec{b}, \vec{c})$. as shown in Fig. 25. The c axis is taken along the chain ($|\vec{c}| = 5.0084(2)$A), the b axis is perpendicular to the chain in the plane of the zigzag chain ($|\vec{a}| = 14.1742(6)$A) and the a axis is perpendicular to the plane ($|\vec{b}| = 5.7583(2)$A).[22]

The shape of a chain is determined by the chain lengths, ℓ_1 and ℓ_2, of bonds and the angles between them, ϕ as shown in Fig. 26. For this chain, the geometrical parameters have been estimated as $\phi = 106.46°$, $\ell_1 = 3.073$A and $\ell_2 = 3.178$A.[22] Recently Taniguchi et al. have made various measurement of this material.[22, 23, 29] In particular, they made experiments on the dynamical shift of ESR resonant frequency of this material.[29] Throughout this chapter we fix the frequency of the oscillation field H_1 to be 9GHz.The unit of the field is Tesla [T].

The spin-spin interaction is written as

$$\mathcal{H}_0 = \sum_{i=1,N/2} 2J_{\rm AF}(S^x_{2i-1}S^x_{2i} + S^y_{2i-1}S^y_{2i} + R_F(S^z_{2i-1}S^z_{2i}))$$

$$- 2J_{\rm F}(S^x_{2i}S^x_{2i+1} + S^y_{2i}S^y_{2i+1} + R_{\rm F}(S^z_{2i}S^z_{2i+1}))). \qquad (5.1)$$

The coupling constants of this chain are determined to be $2J_{\rm F} = 121.3$K and $J_{\rm AF} = 51.4$K [22] but which bond is ferromagnetic is not yet known.

5.2 Dynamical susceptibility

We study the dynamical susceptibility of the model (5.1). We have to determine the parameter of the system. The parameters for the dipole-dipole interaction is determined from the geometrical structure. Here we adopt the dipole-dipole interaction only between the nearest neighbor (nn) pairs. We have compared results of only nn pairs with those of nn and next nn pairs and we found very little difference between them. We set the short bond to be antiferromagnetic and the long bond to be ferromagnetic. We have also found little difference in alternate choice of the bonds.

The shift of the resonance is sensitive to the anisotropy. But first we consider the isotropic case, i.e., $R_F = 1.0$, $R_F = 1.0$. Thus the shift comes from only the dipole-dipole interaction. The temperature dependence of the shift for this case is given in Fig. 27. The marks and lines in Fig. are corresponding to Case1-Case6, as Table 24. Hereafter we use this table.

Here we compare the data at high temperatures with those of experiments because the shifts in experiments at low temperatures maybe affected by various unknown interactions and is difficult to be analyzed.

We quote the relevant experiment results in Fig. 28. There, the g value shift (see below) is shown. This experiment performed in four geometrical configurations (Case1 - Case4 in Fig. 9).

As we had already noted, if the spin-spin interaction has no SU(2) symmetry, we can detect the resonance frequency shift from the paramagnetic resonance. Δg denotes the shift of g value from g_e. The relation between Δg and ΔH is shown as follows.

$$\begin{aligned} g &\rightarrow g + \Delta g \\ &= g \times \frac{H_0}{H_0 + \Delta H} \simeq g - g\frac{\Delta H}{H_0} \end{aligned} \tag{5.2}$$

So, if ΔH is positive, $\Delta g = g - 2.0$ become negative.

The sign of the shift is always negative, which agree with the experiment. But, this result is not satisfactory, because relative relation of the amplitudes of shifts for the 4 geometrical configurations does not agree with that of the experiments. Here the order of the amplitude of the shift is (Case1, Case2, Case4 and Case3) while, in the experiment, the order is (Case1, Case3, Case2 and Case4). In particular, the amplitude of the dynamical shift for $H_0 \parallel$c is behaves opposite way.

In order to find the case which gives the same order as that in the experiment, we variate the anisotropy terms, $R_{\rm F}$ and $R_{\rm AF}$. First we change $R_{\rm F}$ and $R_{\rm AF}$ together. For example, when we decrease $R_{\rm F}$ and $R_{\rm AF}$, which cause the XY anisotropy for both bonds, (i.e., $1 > R_{\rm F} = R_{\rm AF} \geq 0.990$), we find that the shift moves in worse way. Next we study the cases of Ising anisotropy, (i.e., $1 < R_{\rm F} = R_{\rm AF} \leq 1.008$). Then we find the order of Case3 and Case4 exchanged to agree with that of the experiment, but the amplitude of Case1 and Case2 become small and the order is exchanged. Thus we change the anisotropies of the

ferromagnetic bond and antiferromagnetic bond independently. Scanning the parameter, we find that the combination

$$R_{\rm F} = 1.003 \quad \text{and} \quad R_{\rm AF} = 0.996$$

gives a good agreement.(Fig. 29)

5.3 ESR of zigzag chain with Dzyaloshinsky-Moriya interaction

As we mentioned, the Dzyaloshinsky-Moriya(DM) interaction

$$\mathcal{H}_{\rm DM} = \sum_{ij} \vec{\rm d}_{ij} \cdot [\mathbf{S}_i \times \mathbf{S}_j] \tag{5.3}$$

also causes the shift of the resonance frequency. It is, however, difficult to determine the parameters $\{d_{ij}\}$ by fitting the data because of so many parameters. Thus here we investigate general tendency of Dzyaloshinsky-Moriya interaction effect.

Even we consider only nearest neighbor pairs, there are six parameters: i.e. $\vec{d_f} = (dx_f, dy_f, dz_f)$ and $\vec{d_a} = (dx_a, dy_a, dz_a)$, for ferromagnetic bonds and for antiferromagnetic bonds, respectively.

Here we investigate the cases

$$\begin{aligned}[(dx_f, dy_f, dz_f), (dx_a, dy_a, dz_a)] = \ & [(1,0,0)(0,0,0)],\ [(0,1,0)(0,0,0)], \\ & [(0,0,1)(0,0,0)],\ [(0,0,0)(1,0,0)], \\ & [(0,0,0)(0,1,0)],\ [(0,0,0)(0,0,1)]. \end{aligned} \tag{5.4}$$

The static field H_0 is fixed to be 9GHz and the unit of $\vec{d}$ is Kelvin. A typical temperature dependence of the shift is shown in Fig. 30. Here we found that the shift is classified into the following pairs: (Case1, Case6), (Case, Case4), and (Case3, Case5). This means that the shift depends on whether the oscillating field H_1 is parallel to the direction of $\vec{d}$ and the direction of H_0 is not important. Furthermore the shift in ,[(0,1,0)(0,0,0)] and [(0,0,1)(0,0,0)] are almost the same to the Fig. 30, if we regard the axis of $\vec{d}$ as the x direction. If we put DM interaction in the antiferromagnetic bond, the temperature dependences are found different from the ferromagnetic case. But the fact that the shift depends on whether the oscillating field H_1 is parallel to the direction of $\vec{d}$, or not holds as well as the ferromagnetic case. Temperature dependence of the shift for [(0,0,0)(1,0,0)] is shown in Fig. 31. Here we see that the shift is much bigger in the antiferromagnetic case. The cases where H_1 is parallel to $\vec{d}$ the temperature dependence is similar in both ferromagnetic case and antiferromagnetic case. We also studied the case [(1,0,0)(1,0,0)], etc. and find the shift appears as the summation of the shifts for [(1,0,0)(0,0,0)] and [(0,0,0)(1,0,0)]. In the above cases the shift is determined almost only by DM interaction. Thus the amount of 1K for $\vec{d}$ is considered to be strong.

We also investigated $\vec{d}$ with smaller values. We find a sooth change from DM free case. We found that the effect of DM interaction is stronger when $\vec{d}$ is perpendicular to the c axis than the parallel cases.

The magnitude of the Dzyaloshinsky-Moriya interaction is roughly estimated[25, 1]

$$|\vec{d}| \simeq \frac{\Delta g}{g} J.$$

An isotropy effect is roughly estimated [25, 1]

$$\Delta J \simeq (\frac{\Delta g}{g})^2 J.$$

Using these relations and the previous chapter results as $(0.004) = (\Delta g/g)^2$, we can estimate as

$$d \simeq 0.06J \simeq (25 \text{ or } 60) \times 0.06 \simeq 1.54K. \tag{5.5}$$

In the experimental results, there are no such a large shift as we had obtain for $d = 1.0$K, so Eq. (5.5) gives overestimation. This fact is not strange because $|\vec{d}|$ becomes small if the system shape has some symmetries.

We also investigate the case the magnitude of $|\vec{d}|$ is small, *i.e.* $|\vec{d}| = 0.1$K. We can see the smooth change from the no DM effect case. And we also conclude that the DM effect became more weak if $\vec{d}$ is orthogonal to c axis comparing from the case which $\vec{d}$ is parallel to the c axis.

Case1	$H_0 \parallel \vec{a}$, $H_1 \parallel \vec{c}$	solid line
Case2	$H_0 \parallel \vec{a}$, $H_1 \parallel \vec{b}$	dashed line
Case3	$H_0 \parallel \vec{c}$, $H_1 \parallel \vec{a}$	dotted line
Case4	$H_0 \parallel \vec{c}$, $H_1 \parallel \vec{b}$	$\diamond$
Case5	$H_0 \parallel \vec{b}$, $H_1 \parallel \vec{a}$	$\blacklozenge$
Case6	$H_0 \parallel \vec{b}$, $H_1 \parallel \vec{c}$	$\square$

Fig. 24: Six Configurations.

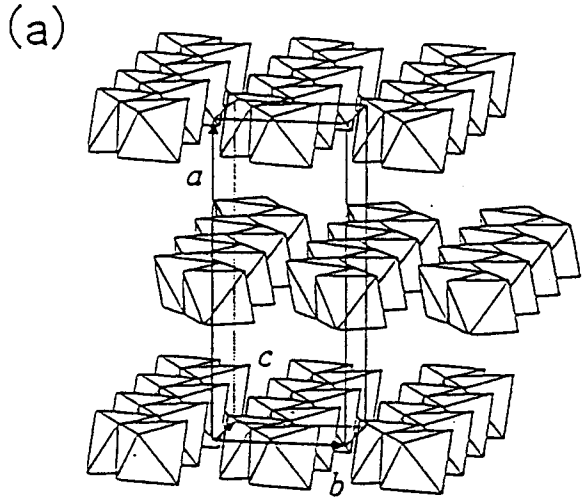

Fig. 25: Zigzag chain of $Cu_{0.9}Zn_{0.1}Nb_2O_6$[22].

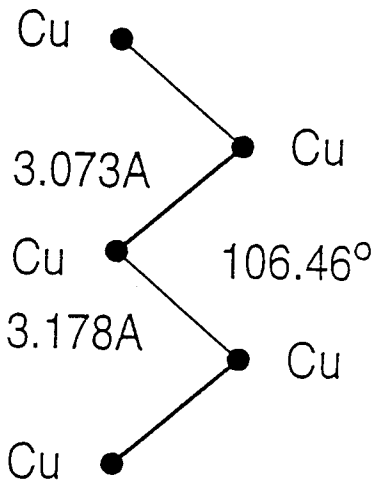

Fig. 26: The space structure of the zigzag chain, $Cu_{0.9}Zn_{0.1}Nb_2O_6$.

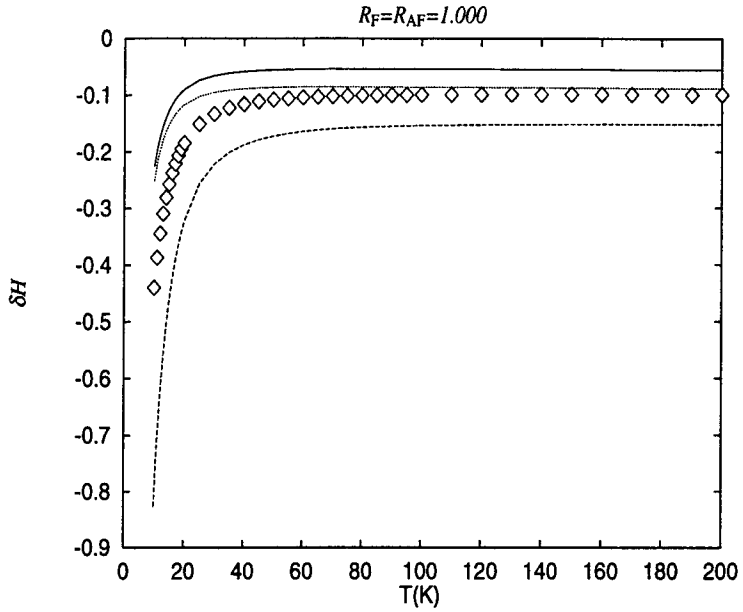

Fig. 27: Temperature dependent of the shift of the resonant field ΔH of the isotropic zigzag chain. δH is a normalized shift : $\Delta H/H_0$. Marks notations and geometrical configurations are shown in Fig. 9 and 24. For Case1 to Case4.

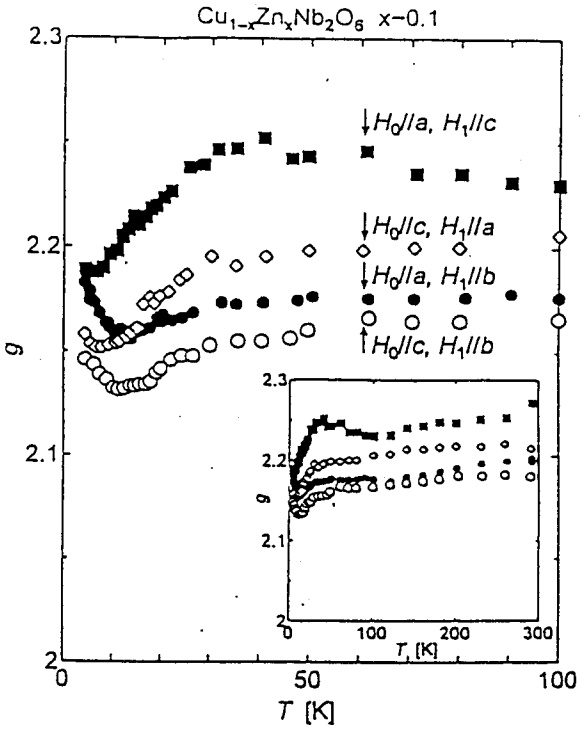

Fig. 28: The temperature dependence of the shift of the g value in $Cu_{0.9}Zn_{0.1}Nb_2O_6$. Quotation from the Taniguchi *et.al.* 's data [29]. ○, ◇, • and □ correspond with Case4, Case3, Case2 and Case1.

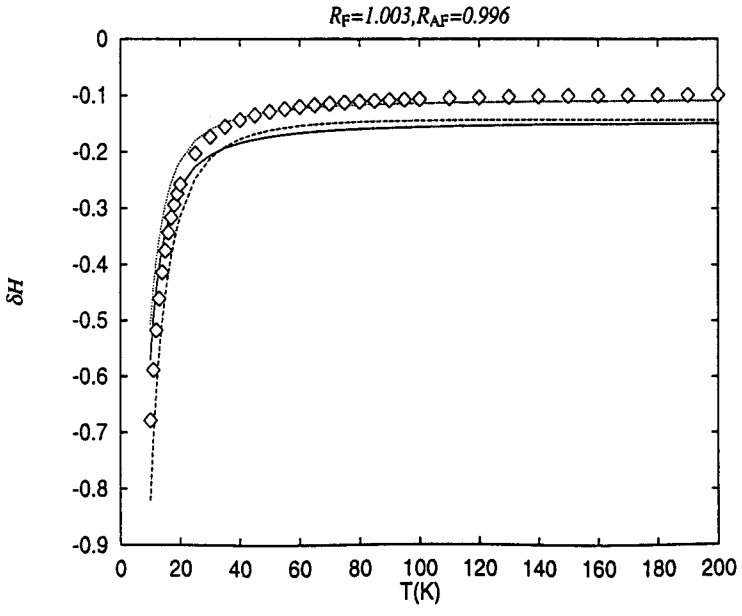

Fig. 29: Dynamical shift for the choice of the parameter: $R_F = 1.003$ and $R_{AF} = 0.996$. Dynamical shifts order agrees with Taniguchi *et al.* 's measurement.

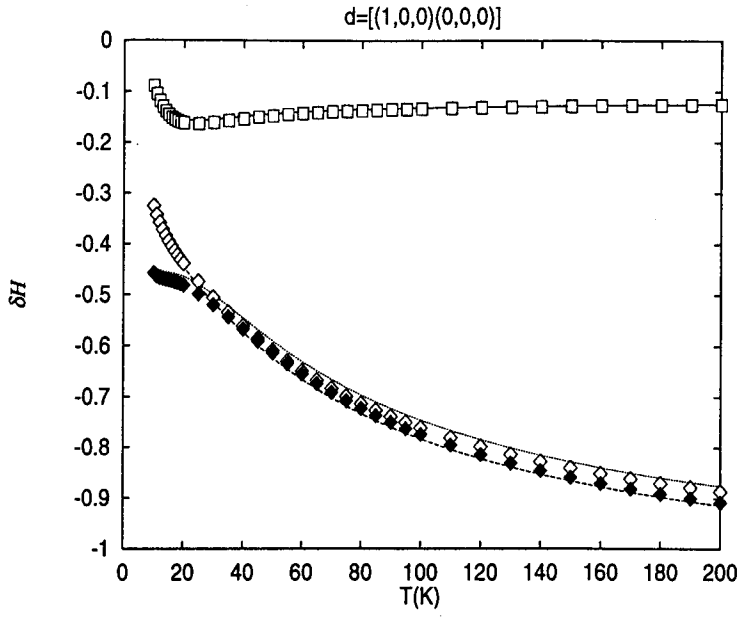

Fig. 30: Dynamical shift for the case with Dzyaloshinsky-Moriya interaction with $\vec{d}$ =[(1,0,0)(0,0,0)]

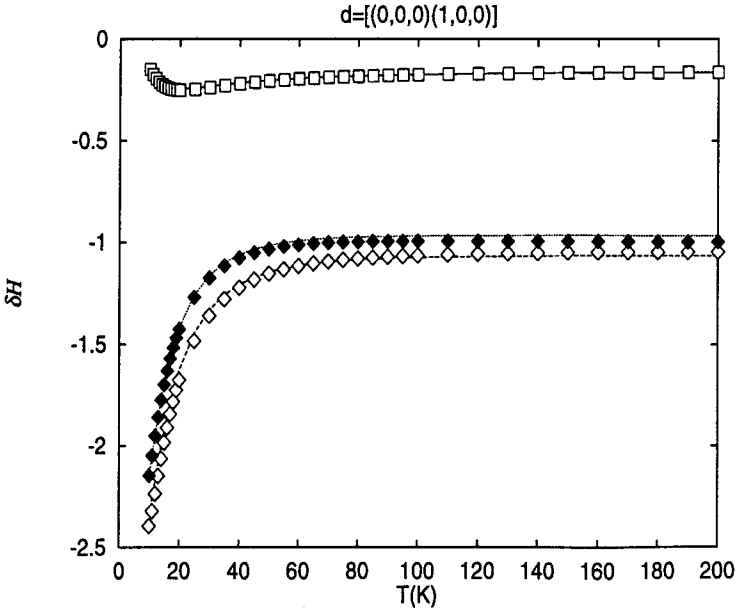

Fig. 31: Dynamical shift for the case with Dzyaloshinsky-Moriya interaction with $\vec{d}$ =[(0,0,0)(1,0,0)]

Chapter 6

New Method to Determine Structure of Interaction

As mentioned in chapter 5, there are a ferromagnetic bond and an antiferromagnetic bond in $Cu_{0.9}Zn_{0.1}Nb_2O_6$. The length of them are ℓ_1=3.073A or ℓ_2=3.178A. However there are no method to determine which bond is ferromagnetic. Because the lengths of the bonds are very close, it is difficult to distinguish them in macroscopic measurements. Here we would propose a new method making use of the dynamical shift to determine which bond is ferromagnetic. As we saw in th previous chapter, dynamical shifts in the 6 geometrical configurations are not sensitive which bonds is ferromagnetic. On the other hand, we expect a significant difference between the shift of the case where the static field is parallel to the ferromagnetic bond and that of the case where the static field is parallel to the antiferromagnetic bond.

In Figs. 32 and 33, we show the temperature dependence of the shift for the parameters found in the previous chapter. Here we find a definite difference in the case changing H_1, while there is little difference when we change H_0. Thus the dynamical shift with H_1 can be a new method to determine which bond is ferromagnetic and thus the other is antiferromagnetic. We should point out that this method works only on a crystal, but not powder. Fortunately, crystal of $Cu_{0.9}Zn_{0.1}Nb_2O_6$ is available and we expect that such measurement will be done. However as will be mentioned in the proceeding chapter, in order to predict the difference we need to know the interaction correctly. Beside the dipole-dipole interaction and the anisotropy, magnetic systems generally have various other sources for the shifts, such as Dzyaloshinsky-Moriya (DM) interaction. Furthermore the anisotropy of the g-factor is also anther important parameter in real materials. Although the dipole-dipole interaction can be determined from the geometrical information, parameters for other interactions must be known from other informations or determined by fitting experimental data. In fact we did a fitting the anisotropy parameters in the previous chapter setting DM interaction to be 0, which is not satisfactory. In practice, it is difficult to know all the parameters. However the idea to determine the structure of interaction through the dynamical shift will provide a new kind of informations for the parameter and we hope that this measurement will be

done and find the difference in the shift.

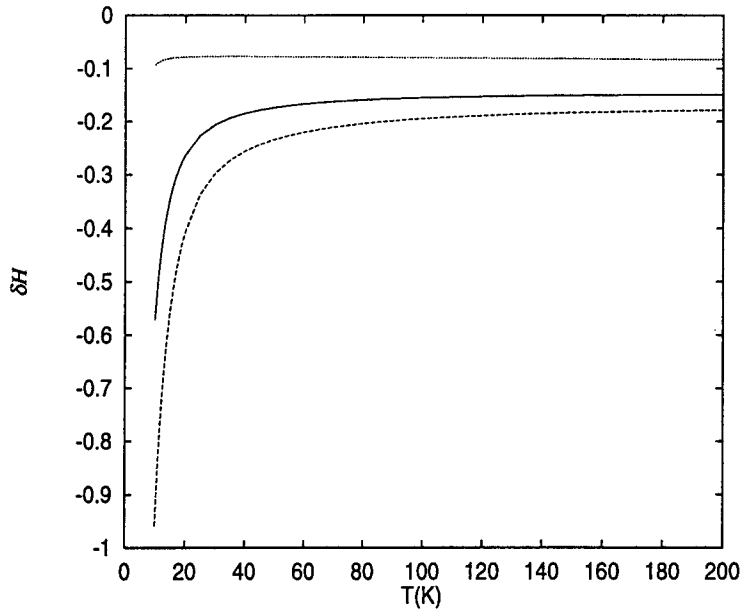

Fig. 32: Dynamical shift for changing H_1: The dashed line denotes the case where H_1 parallel to the ferromagnetic bond, the dotted line the case where H_1 parallel to the antiferromagnetic bond, and the solid line where H_1 parallel to the c axis.

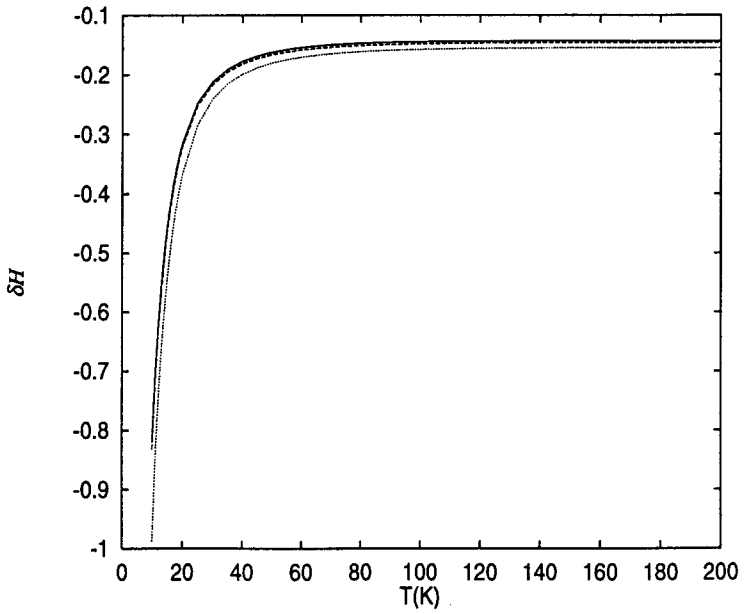

Figs. 33: Dynamical shift for changing H_0: The dashed line denotes the case where H_0 parallel to the ferromagnetic bond, the dotted line the case where H_0 parallel to the antiferromagnetic bond, and the solid line where H_0 parallel to the c axis.

Chapter 7

ESR in the system with strong quantum fructuation

In this chapter, we investigated the dynamical shifts in one dimensional $S = 1/2$ alternating bond chain. As explained in chapter 1, $S = 1/2$ ferro-antiferro magnetic alternating bond chain exhibits various quantum phases in the ground state when we control the bonds strength. There are four phases, *i.e.*, Haldane phase, Néel phase, like Dimer phase state, and Large D phase.

We investigated the system which has a set of ferro-anntiferro magnetic bonds corresponding to typical quantum phases, respectively. We calculated the temperature dependence of the shift of resonance magnetic field $\Delta H(T)$. Namely, for each system, we studied the shift with six geometrical configurations denoted by static field $\mathbf{H}_0$, resonance field $\mathbf{H}_1$, and along chain axis c.These configurations are shown in Fig. 9.

To see the shift of resonance in such quantum phases, we should take into account the non-symmetric spin-spin interactions, such that dipole-dipole interaction. For all cases, we take into account dipole-dipole interaction setting the bond length to be $l = 3.0$A.

The system Hamiltonian is given by Eq. (5.1). To check the effect of spatial structure of chain, we varied the angle between bonds. We set the angle change from linear chain case ϕ, for example, $\phi = 0$ for linear chain case. We varied ϕ as 0(linear chain case), 0.1π, 0.2π. We assume the zigzag structure lying in the XY plane. Strength of static field H_0 are 10, 20, and 50GHz. We investigated with the temperature range form 0.1K to 20K. We do not take into account Dzyaloshinsky-Moriya interaction.

7.1 Explanation about each quantum phase

7.1.1 The Haldane phase

For the strong ferromagnetic bonds, spins in both sides of the ferromagnetic bond couple and make a $S = 1$ spin. These $S = 1$ spins interact weakly with antiferromagnetic bond. So the system have the nature of one dimensional antiferromagnetic chain and thus the

Haldane phase in the ground state. As a typical set of parameters, we take $J_F/J_{AF} = 5.0$, $J_{AF} = 1.0$K, $R_F = R_{AF} = 1.0$.

7.1.2 The Néel phase

Due to the strong Ising anisotropy in the antiferromagnetic bond, the effective $S = 1$ likely align "antiparallel" each other in the z direction. The spin system is in the Néel state in the ground state. Here, we set $J_F/J_{AF} = 5.0$, $J_{AF} = 1.0$K, $R_F = 1.0$, $R_{AF} = 5.0$.

7.1.3 The Dimer phase like state

In this case, the strong antferromagnetic bond makes valance bond (singlet pair) with spins in both side of the bond. The physical picture is that the valance bonds interacts with weak ferromagnetic interaction. As noted in chapter 1, we can distinguich Dimer state and Haldane phase in $S = 1$ case, so we can define the Dimer phase. But in the $S = 1/2$ bond alternating chain, there are no clear phase transition between Haldane phase and "Dimer phase". We set $J_F/J_{AF} = 0.2$, $J_F = 1.0$K, $R_F = R_{AF} = 1.0$.

7.1.4 The Large D phase

For strong XY type anisotropy of the ferromagnetic bond, the spins both side of the bond tend to be "parallel" to the the XY plane. Conposition of two spins tend to became the state with total spin is 0. It is considered that the term $-D(S_i^z + S_{i+1}^z)^2$ in added to the isotropic hamiltonian. Here i and $i+1$ are the pair of spin site besides a feromagnetic bond. Originally, this term is considered in $S = 1$ case, but we can adopt to the $S = 1/2$ case regarding two spins beside the ferromagnetic bond as one $S = 1$ spin. We set $J_F/J_{AF} = 5$K, $J_{AF} = 1.0$K, and $R_F = 0R_{AF} = 1.0$.

7.2 Dynamical shift in each quantum phase

7.2.1 The Haldane phase

The hamiltonian which is in a Haldane phase in the ground state, has SU(2) symmetry. Therefore, the shift of the resonance field come from the diple-dipole interaction term. We start with the linear chain , *i.e.* $\phi = 0$.

In the strong static magnetic field case, *i.e.* $H_0 = 50$GHz, the shift depends on the angle between the static field direction H_0 and chain direction c. When H_0 is orthogonal to c, ΔH appeares positive and when H_0 is parallel to c, ΔH apperes negative. In both cases, the shift magunitude tends to be zero as the temperature T increases (Fig.34). This nature is resemble to the nature of $S = 1/2$ one dimentional antiferromagnetic chain shown in chapter 4.

In weak static magnetic field case, *i.e.*,$H_0 = 10$GHz, almost all of six sifts appears below zero (Fig.35). At $1K$, the tendency of the shift changes. It is considered that this is due to the effect of the gap between the ground state and the first excited state as Fig. 35. The absorption became very small at the low tempareture.

For system symmetry, we can classify the six configurations to three cases. The case $H_1 \parallel c$, the case $H_0 \parallel c$, and other configurations. Each of them has two geometical configulations, which are physically equevalent when $\phi = 0$, so the shift should be exactly same, which has been checked in calculation.

Next, we check the case $\phi = 0.1\pi$ and 0.2π cases. If ϕ is nonzero, the symmetry between the b axis and a axis breaks. We observed the effect of this symmetry beraking. For a strong field case(H_0 =50GHz) , the shift depends mainly on the direction of the static field H_0. Shift in $\phi = 0.2\pi$ case is shown in Fig. 36.

7.2.2 The Néel phase

In all six configulations, the resonance shift ΔH appears negative. Moreover, the magunitude of the shift is very large compareing with the Haldane phase. It is considered that this is because that the shift is very sensiteve to the anisotropy of the hamiltonian compareing from dipole-dipole interaction, as seen in chapter 5.

In the week static magnetic field case (H_0=10GHz), we can roughly classify the shifts into two groups, one is $H_1 \parallel z$, z axis is the Néel direction, and the other is case with H_1 (Fig.37). We conclude the shits is sensitive to the H_1 direction. This tendency holds when H_0 is strong such as H_0=50GHz(Fig.38). In all cases, the tendency of the shift depends little on the ϕ chang. It is considered that this is because the contribution of dipole-dipole interaciton is rather small comparing the contribution of anisotropy of the exchange integrals.

7.2.3 Dimer like phase state

In this type of the system, there is a gap between the ground state and the first excited state. The spin-spin interaction has SU(2) symmetry and the shift of the resonance is infulenced only by the dipole-dipole interaction term. These charactoristics are the same as the Haldane system case and the tendency of the dynamical shift apperes in the same way.

For example, when $\phi = 0$ and the magnetic field is weak, *i.e.* H_1=10GHz, all the shift appear negative. And in the strong magnetic field case, *i.e.* H_0 =50GHz, the sign of the sift depends on whether the H_0 direction is orthogonal or parallel to the chain direction as seen in Fig. 39. Last point is that all the shifts tend to 0 in the high tempareture limit in strong static field case.

Futhermore, this state, not only in weak field case ($H_1 = 10$GHz) but also in strong field case (H_0=50GHz), the large shift is observed at $T < 2$K, perhaps due to the enrgy gap between the ground state and the first exited state.

When the space structure of the chain is zigzag, for example in the $\phi = 0.2\pi$ case, the system symmetry between the a axis and the b axis breaks. So the shifts which appere in the same direction and the same magnitude in the case of $\phi = 0$ split in the zigzag structure (Fig. 40).

7.2.4 Large D phase

In this phase, shift of resonance appears negative in all cases. The shift amplitude is very large, if we compare with the Haldane phase case.

In Fig. 41, the tempareture dependence of the shift is shown for $\phi = 0$ and H_0=10GHz. We can classify the 6 shifts into two groups, the former are H_1 is parallel to the XY plane and latter group is H_1 is orthogonal to the XY plane. When H_1 is parallel to the a axis of the crystal, observed shift is rather small comparing with other cases. In the strong H_0 case, *i.e.* $H_0 = 50$ GHz, the almost same nature is observed as the weak H_0 case, though magnitude in the formar case is rather small comparing with the latter(Fig. 42).

The qualitative nature of the shift does not change with the change of ϕ. The reason of this is that the effect of the dipole-dipole interaction to the shift is rather small comparing with the anisotropy effect.

7.3 General remarks

Dynamical shift has studied with the systems which ground state is in the Haldane phase, the Néel phase, Dimer like phase state, and Large D phase. Here, we summarize the general tendency. Roughly speaking, we can separate 4 cases into 2 groups. The first group is the spin systems with SU(2) symmetry. They have the nature likes $S = 1/2$ antiferromagnetic chain. The ground state of this group is in the Haldane phase or the Dimer like phase. In the second group is the spin systems without SU(2) symmmetry. They have the large shift due to the anisotropy of exchange interaction comparing with the first group. The ground state of this group is in the Néel phase or large D phase. The former group's shift is sensitive to the angle ϕ and the latter group's shit is insensitive.

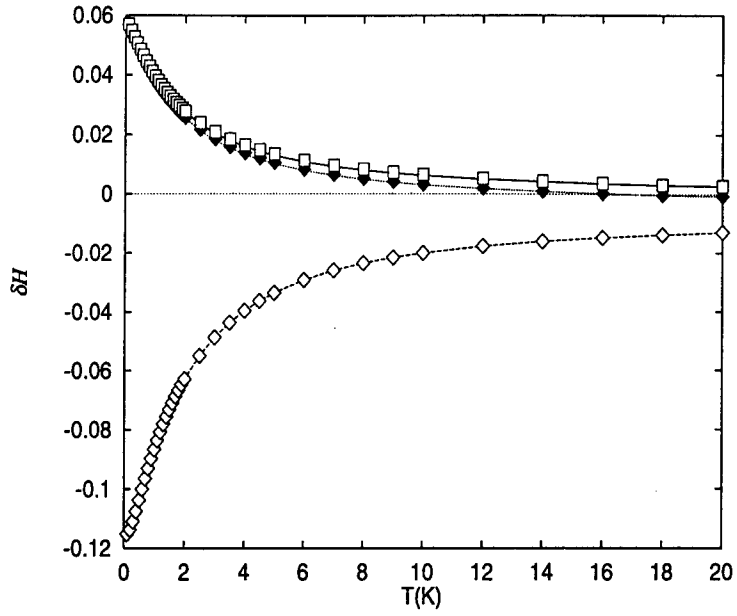

Fig. 34: Dynamical shift in the system which ground states is in a Haldane phase. $H_0 = 50$GHz and $\phi = 0$. ΔH, the shift of resonance field is shown in a vertical axis. K , the temperature is shown in a horizontal axis.

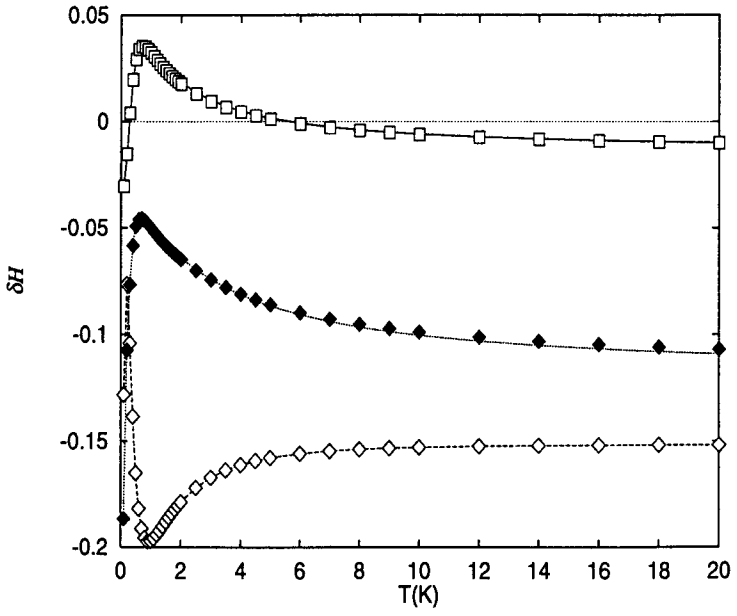

Fig. 35: Dynamical shift in the system which ground states is in a Haldane phase. $H_0 = 10$GHz and $\phi = 0$. ΔH, the shift of resonance field is shown in a vertical axis. K , the temperature is shown in a horizontal axis.

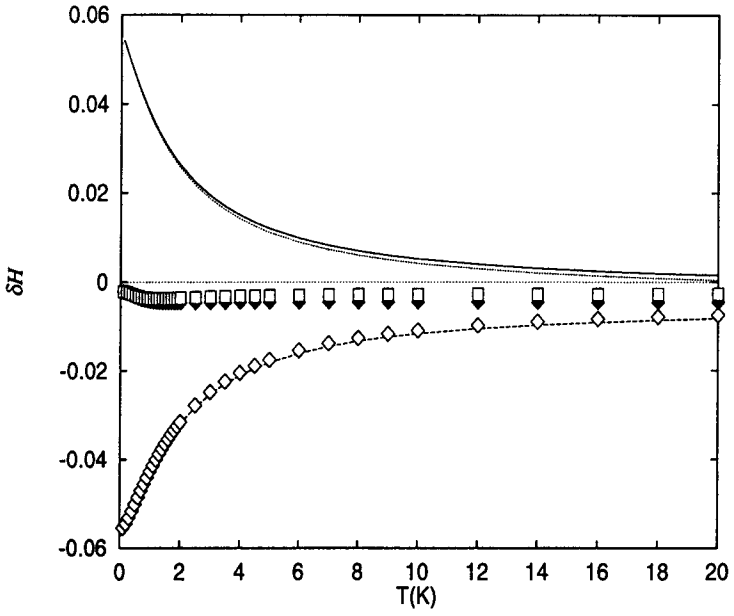

Fig. 36: Dynamical shift in the system which ground states is in a Haldane phase. $H_0 = 50$GHz and $\phi = 0.2\pi$. ΔH, the shift of resonance field is shown in a vertical axis. K , the temperature is shown in a horizontal axis.

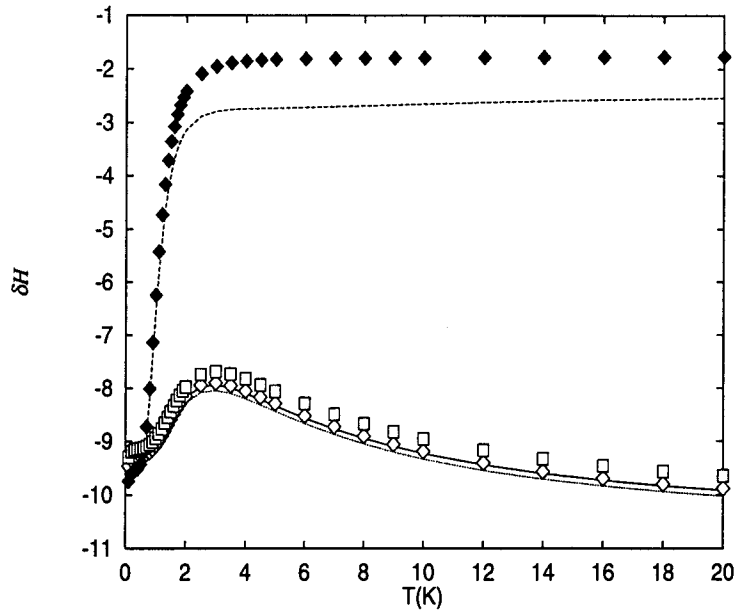

FIg. 37: Dynamical shift in the system which ground states is in a Néel phase. $H_0 = 10$GHz and $\phi = 0$. ΔH, the shift of resonance field is shown in a vertical axis. K , the temperature is shown in a horizontal axis.

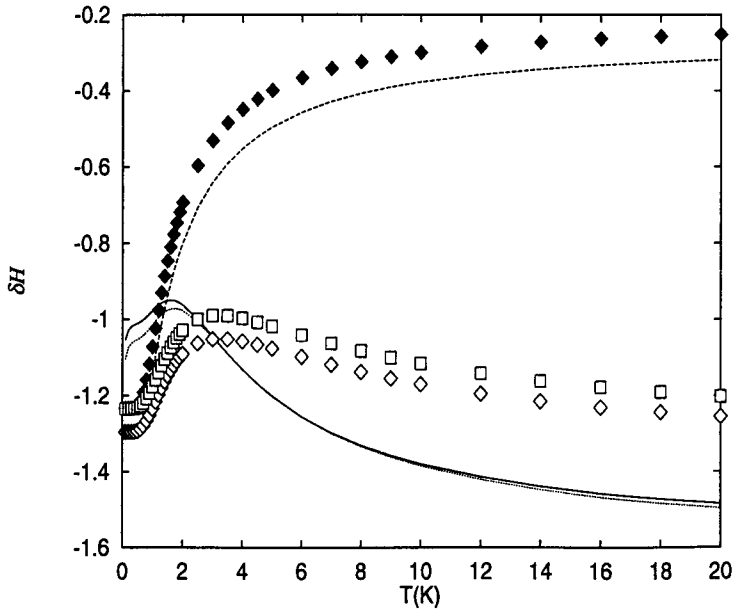

Fig. 38: Dynamical shift in the system which ground states is in a Néel phase. $H_0 = 50$GHz and $\phi = 0$. ΔH, the shift of resonance field is shown in a vertical axis. K , the temperature is shown in a horizontal axis.

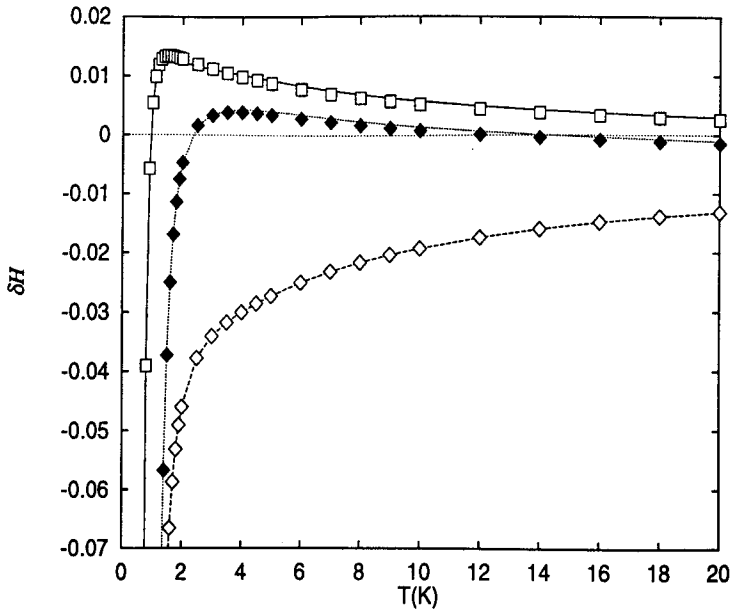

Fig. 39: Dynamical shift in the system which ground states is in a Dimer phase like state. $H_0 = 50\text{GHz}$ and $\phi = 0$. ΔH, the shift of resonance field is shown in a vertical axis. K , the temperature is shown in a horizontal axis.

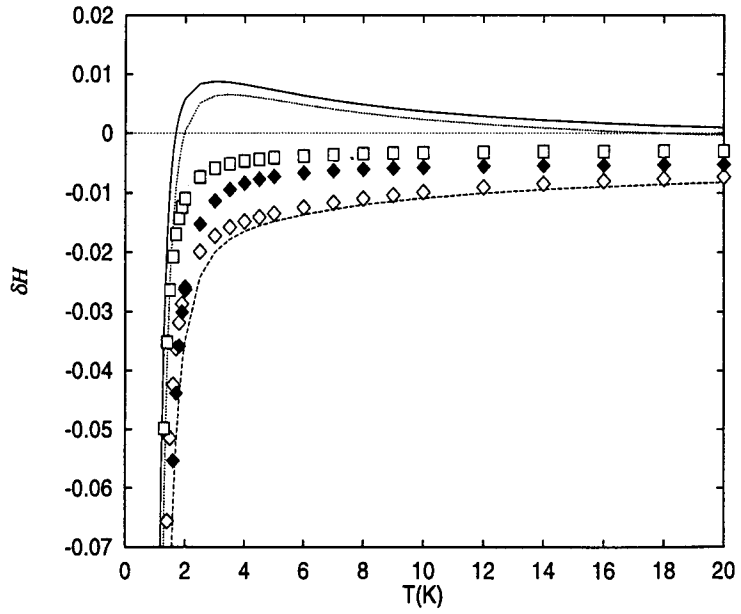

zig

Fig. 40: Dynamical shift in the system which ground states is in a Dimer phase like state. $H_0 = 50\text{GHz}$ and $\phi = 0.2\pi$. ΔH, the shift of resonance field is shown in a vertical axis. K , the temperature is shown in a horizontal axis.

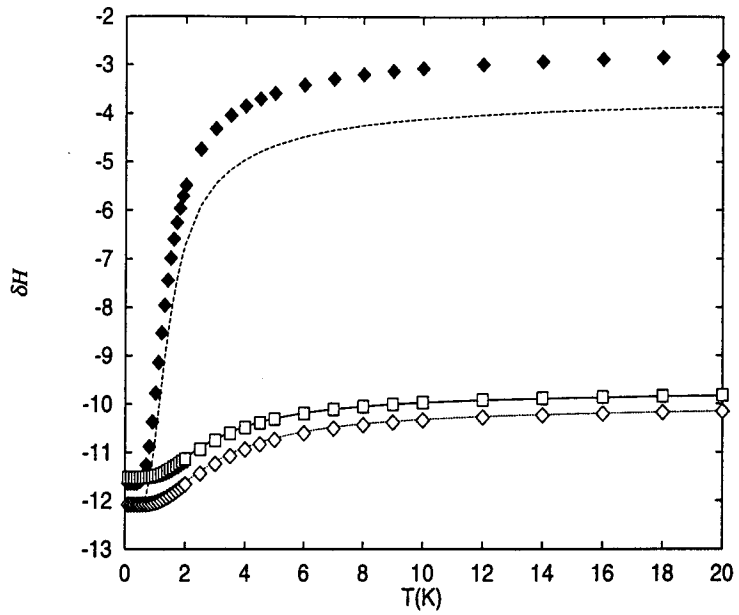

Fig. 41: Dynamical shift in the system which ground states is in a large D phase. $H_0 = 10$GHz and $\phi = 0$. ΔH, the shift of resonance field is shown in a vertical axis. K , the temperature is shown in a horizontal axis.

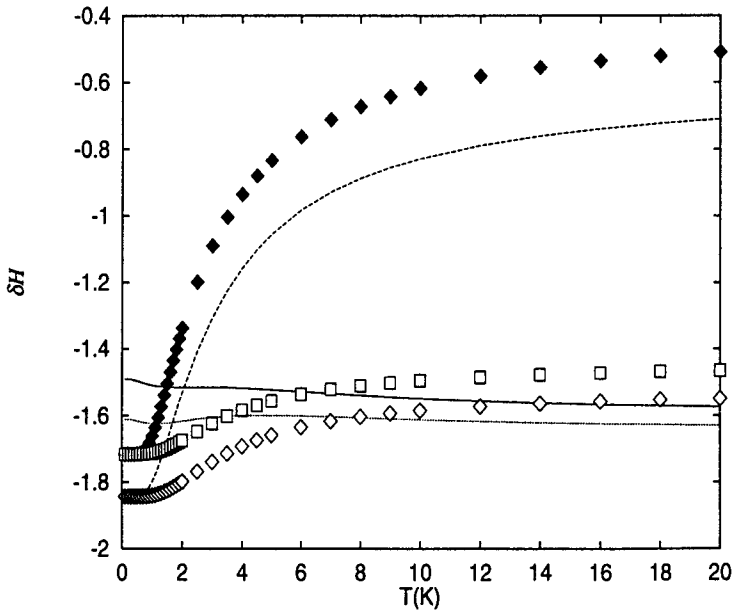

Fig. 42: Dynamical shift in the system which ground states is in a large D phase. $H_0 = 50$GHz and $\phi = 0$. ΔH, the shift of resonance field is shown in a vertical axis. K , the temperature is shown in a horizontal axis.

Chapter 8

Conclusion

8.1 The obtained results

We proposed a direct numerical method to calculate the dynamical susceptibility, $\chi''(\omega)$, in strongly fluctuating quantum systems, using Kubo formula. Calculating the spin-spin correlation function in a small system numerically exact,we can obtain the absorption line shape due to dipole-dipole interaction and other spin-spin interactions. We used histogram representation of the line shape, because original result is the assembly of the delta function. We calculated dependence of the line shape on the geometrical configuration of chain and fields which is caused by the dipole-dipole interaction.

We performed this method in $S = 1/2$ one dimensional quantum spin systems. We calculated the resonance shift from the paramagnetic resonance by averaging the absorption line and we reproduce the results of Nagata-Tazuke[7] for temperature dependence of dynamical shift. We also investigated the effect of anisotropy, the effect of the magnetic field strength, geometrical effect, on the dynamical shift. In particular, we found that the resonance shift is sensitive to anisotropy of exchange interaction.

We also investigated the relevant model of the material, $Cu_{0.9}Zn_{0.1}Nb_2O_6$[29]. This model is a $S = 1/2$ one dimensional zigzag chain. We investigated dynamical shift of the chain, and fitting the anisotropy parameter of bond for each bond, and finally reproduced same properties of the experimental results. We also investigated Dzyaloshinsky-Moriya interaction effect on the dynamical shift.

$Cu_{0.9}Zn_{0.1}Nb_2O_6$, has two kinds of bond,one of them is a little longer than the other. But we can not determine which bond is ferromagnetic in present macroscopic experiments. We calculated the dynamical shift when the oscillating field is parallel to ferromagnetic bond and when also the oscillating field is parallel to the antiferromagnetic bond. We found a distinguishable difference between them. We proposed that comparing these two dynamical shifts, we determine which bond is ferromagnetic and which bond is antiferromagnetic.

This method for structure determination is a new type of method, where combination of experiments and numerical calculation is profitable to study the material nature.

We also investigated the various $S = 1/2$ spin systems which are in various quantum phases in the ground states, such as the Haldane phase, the Dimer like phase, the Nèel phase, and the Large D phase. We investigated the dynamical shift of such phases. We investigated the effect of field strength, geometrical configuration of chain and fields, and the effect of the chain shape to the shift, in each phases.

8.2 Further problems

We summarize the further problems.

Study on various quantum $S = 1/2$ spin chains

There are many materials investigated experimentally using ESR. For example, $(CH_3)_2CHNH_3CuCl_3$[27], $S = 1/2$ zigzag chain was investigated by Manaka *et al.*. Powder sample of $CuCl_2 \cdot 2Dx$ was investigated by Ajiro *et.al.*, which is considered $S = 1/2$ trimer with ferromagnetic-ferromagnetic-antiferromagnetic interaction. The impurity effect[41],is also interesting. The ladder model is also interesting and can be calculated by our method.

Study on quantum liquid states, especially $S = 1$ case

In this thesis, we investigated quantum liquid state using $S = 1/2$ bond alternating chain, but the calculation in $S = 1$ system is possible and we expect to obtain more detailed nature of quantum liquid states. There are many experimental and theoretical studies on one dimensional $S = 1$ spin systems with interest in Haldane conjecture. It is interesting to study the effect of impurity and the effect of the open boundary, on ESR line shape and resonance shift.

Quantum relaxation phenomena

Concerning the quantum relaxation, several ESR measurement are done, i.e. Mn_{12} and Fe_8[40]. Dynamical shift in Such systems is also interesting.

Dipole-dipole interaction effect from distant sites, Ferromagnetic resonance.

Dipole-dipole interaction is a long range force, and we should take this into account for detailed research. With our method, we can consider the dipole-dipole interaction with half system size distance. It is interesting to investigate effect from distant sites. We desire to investigate the ferromagnetic resonance taking a demagnetizing field into account.

Absorption line shape study

As to the detail line shape, such as the Gaussian or Lorentzian or intermediate one is an interesting problem. For this, the study on larger systems is required.

Development of the method to determine the structure constants

We want to establish the practical procedure to determine physical properties of material comparing the experimental result and the numerical calculation, examining the ESR dynamical shift. If it is reasonable to assume the shape of the spin-spin interaction can be represented only with nearest neighbor spin pairs, the number of the unknown parameters are only nine(see appendix B). In this sense, nine kinds of experiments and numerical calculation of the shift can determine the constant.

Chapter 9

Acknowledgment

The author would like to thank to the Professor Seiji Miyashita for general discussion and encouragement. In performing the numerical simulation, the author thanks to Mr. Akira Ogasahara for cooperation. And we thanks to the member of the Miyashita laboratory and Akutsu laboratory, and Akiyoshi Kuroda in Nagoya, to leave me comfortable state. We also thanks to Dr. Satoshi Taniguchi, Professor Masatoshi Sato, Professor Isao Yamada, Professer Yoshitami Ajiro, for showing us unpublished experimental data.

Chapter 10

Appendix

Appendix A : Derivation of the Kubo fomula

Here, We will derive the Kubo fomula.

We will make a perturbation treatment to a time dependent external field. The perturbation term $\mathcal{H}'$ is for

$$\mathcal{H}' = -AF(t). \tag{10.1}$$

The Hamiltonian of the system $\mathcal{H}$ is

$$\mathcal{H} = \mathcal{H}_0 + \mathcal{H}' \tag{10.2}$$

This means that the external field $F(t)$ is conjugate to a physical quantity A. We assume the system is in equilibrium at the initial time, $t = -\infty$, for the hamiltonian is $\mathcal{H}$. The density matrix ρ_0 at a temperature T is given by

$$\rho_0 = \rho(-\infty) = \frac{\mathrm{e}^{-\beta\mathcal{H}_0}}{\mathrm{Tre}^{-\beta\mathcal{H}_0}}, \tag{10.3}$$

where $\beta = 1/K_{\mathrm{B}}T$. The expectation value of operator B is given as

$$\langle B \rangle \equiv Tr[\rho_0 B]. \tag{10.4}$$

The external field $F(t)$ is applied to the system after that.

We think the time evolution of dencity matrix is given by

$$i\hbar\frac{\mathrm{d}}{\mathrm{dt}}\Delta\rho(t) = [\mathcal{H}_0 + \mathcal{H}', \rho_0 + \Delta\rho(t)] \tag{10.5}$$

We regards $\mathcal{H}'$ is sufficiently small comparing with $\mathcal{H}_0$. Thus we consider the change $\Delta\rho(t)$ in the first order of $\mathcal{H}'$. Neglecting the seconed order quantity $[\mathcal{H}', \Delta\rho(t)]$,

$$i\hbar\frac{\mathrm{d}}{\mathrm{dt}}\Delta\rho(t) = [\mathcal{H}_0, \Delta\rho(t)] + [\mathcal{H}', \rho_0]. \tag{10.6}$$

The solution of this equation is

$$\Delta\rho(t) = -\frac{1}{i\hbar}\int_{-\infty}^{t} \mathrm{e}^{-i(t-t')\mathcal{H}/\hbar}[A,\rho]\mathrm{e}^{i(t-t')\mathcal{H}/\hbar}. \tag{10.7}$$

With the external field , we obtain the time dependence of a physical quantity B. Here we asume $\langle B\rangle$ in the absence of the field is 0. The time dependence of $\langle B\rangle$, which is written $\Delta B(t)$, is given as

$$\begin{aligned}\Delta B(t) &= -\frac{1}{i\hbar}\mathrm{Tr}\int_{-\infty}^{t} e^{-i(t-t')\mathcal{H}/\hbar}[A,\rho]\mathrm{e}^{i(t-t')\mathcal{H}/\hbar}BF(t')\mathrm{d}t' \\ &= -\frac{1}{i\hbar}\int_{-\infty}^{t}\mathrm{Tr}[A,\rho]e^{i(t-t')\mathcal{H}/\hbar}B\mathrm{e}^{-i(t-t')\mathcal{H}/\hbar}F(t')\mathrm{d}t' \\ &= -\frac{1}{i\hbar}\int_{-\infty}^{t}\mathrm{Tr}\rho[B(t-t'),A]F(t')\mathrm{d}t' \end{aligned} \tag{10.8}$$

Deriving this equation, we used the relation $\mathrm{Tr}AB = \mathrm{Tr}BA$ with operators A and B. Here,

$$B(t-t') = \mathrm{e}^{i(t-t')\mathcal{H}/\hbar}B\mathrm{e}^{-i(t-t')\mathcal{H}/\hbar}. \tag{10.9}$$

If we set

$$\phi_{BA}(t-t') \equiv -\frac{1}{i\hbar}\mathrm{Tr}\rho[B(t-t'),A], \tag{10.10}$$

Eq.(10.8) becomes

$$\Delta B(t) = \int_{-\infty}^{t}\mathrm{Tr}\phi_{BA}(t-t')F(t')\mathrm{d}t'. \tag{10.11}$$

Substituting $\hbar = 1$,$F(t) = H^z(t)$,$B = A = M^x$ to Eq.(10.10) and Eq.(10.11), and making use of the rotation of operators in the trace,we finally obtain the Eq.(2.39) and Eq.(2.40) as

$$\langle M^z(t)\rangle = \int_{-\infty}^{t}\phi_{xx}(t-t')H^z(t')\mathrm{d}t' \quad (2.39)$$

and

$$\phi_{xx}(t-t') = i\langle[M^x(t),M^x(t')]\rangle \quad (2.40).$$

Appendix B: Hamiltonian with the Pauli Matrix

Here we show the explicit expression of interaction between the spin $\mathbf{S}_i$ and $\mathbf{S}_j$,$h[ij]$ in the Pauli matrix expression which is used in Eq.(3.13).

$$\begin{aligned} h[ij] &= \begin{pmatrix} S_i^x & S_i^y & S_i^z \end{pmatrix}\begin{pmatrix} h_{11} & h_{12} & h_{13} \\ h_{21} & h_{22} & h_{23} \\ h_{31} & h_{32} & 33 \end{pmatrix}\begin{pmatrix} S_j^x \\ S_j^y \\ S_j^z \end{pmatrix} \\ &= (\frac{1}{4}(h_{11}-h_{22}) + \frac{1}{4i}(h_{12}+h_{21}))\sigma_i^+\sigma_j^+ + \\ &\quad (\frac{1}{4}(h_{11}-h_{22}) - \frac{1}{4i}(h_{12}+h_{21}))\sigma_i^-\sigma_j^- + \end{aligned}$$

$$
\begin{aligned}
&(\frac{1}{4}(h_{11}+h_{22})+\frac{1}{4i}(h_{21}-h_{12}))\sigma_i^+\sigma_j^- + \\
&(\frac{1}{4}(h_{11}+h_{22})-\frac{1}{4i}(h_{21}-h_{12}))\sigma_i^-\sigma_j^+ + \\
&\frac{1}{4}h_{33}\sigma_i^z\sigma_j^z + \\
&(\frac{1}{4i}h_{32}+\frac{1}{4}h_{31})\sigma_i^z\sigma_j^+ + (-\frac{1}{4i}h_{32}+\frac{1}{4}h_{31})\sigma_i^z\sigma_j^- + \\
&(\frac{1}{4i}h_{23}+\frac{1}{4}h_{13})\sigma_i^+\sigma_j^z + (-\frac{1}{4i}h_{23}+\frac{1}{4}h_{13})\sigma_i^-\sigma_j^z
\end{aligned}
$$

Now, $\sigma_i^\alpha = 2S_i^\alpha$ and α denotes x, y, or z. And $\sigma^+ = S^x + iS^y$, $\sigma^- = S^x - iS^y$.

Bibliography

[1] M. Date: Electron Spin Resonance (1978) Baifu-kan, and reference there in.

[2] F. D. M. Haldane: Phys. Lett. **A93** (1983) 464-468.

[3] F. D. M. Haldane: Phys. Rev. Lett. **50** (1983)1153-1156.

[4] S. Miyashita, T. Yoshino, and A. Ogasawara: J. Phys. Soc. Jpn. (in press Feb. 1999).

[5] T.Yoshino, A. Ogasawara and S. Miyashita: In preparation.

[6] J. Kanamori and M. Tachiki: J. Phys. Soc. Jpn. **17** (1962) 1384.

[7] K. Nagata and Y. Tazuke: J. Phys. Soc. Jpn. **32** (1972) 337.

[8] R. Kubo and K. Tomita: J. Phys. Soc. Jpn. **9** (1954) 888.

[9] R. Kubo: J. Phys. Sco. Jpn. **12** (1957) 570.

[10] N. D. Mermin and H. Wargne, Phys. Rev. Lett. **17** (1966) 1133.

[11] M. Kikuchi, Y. Okabe, S. Miyashita: J. Phys. S. Jpn. **59** (1990) 492.

[12] S. Miyashita: International Workshop on Quantum Simulations of condenced matter phenomina,8-11 August, World Scientific (1990).

[13] S. Takada:In Quantum Monte Carlo Methods,Springer-Verlag(1987).

[14] F. H. L. Essler, H. Frahm, A. G. Izergin, V. E. Korepin: Commun.Math.Phys.**174**(1995) 191.

[15] Y. Kato, A. Tanaka: J. Phys. Soc. Jpn. **63** (1994) 1277.

[16] M. Yamanaka, M. Oshikawa, S. Miyashita: J. Phys. Soc. Jpn. **65**(1996) 1562.

[17] K. Katsumata, H. Tasaki ed. : Haldane Gap-Macroscopic Quantum Phenomina in Spin Systems, Selected Papers in Physics VIII (1997) The Physcical Society of Japan.

[18] K. Hida : Phys. Rev. B : **46**(1992) 8268.

[19] K. Hida: Computational Physics as a New Frontier in Condensed Matter Research (1995) 187-191.

[20] Y. Natsume, F. Sasagawa, M. Toyoda and I. Yamada: J. Phys. Soc. Jpn. **48**(1980) 50.

[21] Y. Hamano and F. Shibata: J. Phys. C: Solid State Phys. **17**(1984) 4843 and 4855.

[22] T. Nishikawa, M. Kato, M. Kanada, T. Fukamachi, K. Kodama, H. Harashima, and M. Sato: J. Phys. Soc. Jpn. **67** (1998) 1988-1993.

[23] T. Fukamachi, Y. Kobayashi, M. Kanada, M. Kasai, Y. Yashui and M. Sato: J. Phys. Soc. Jpn. **67** (1988) 2107-2111.

[24] I. Dzialoshinsky : J. Phys. Chem. Solids **4** (1958) 241.

[25] T. Moriya : Phys. Rev. Lett.**4** (1960) 228.

[26] Manaka *et. al.* (1998) Meeting Abstracts of the Physical Society of Japan, **53**, Issue 2, Part 3, 588.

[27] H. Manaka, I. Yamada and K. Yamaguchi: J. Phys. Soc. Jpn. **66** (1997) 564-567.

[28] F. Shibata and N. Hashitsume: J. Phys. Soc. Jpn. **44** (1978)1435.

[29] S. Taniguchi M. Kato, K. Kodama, Y. Kobayashi and M. Sato: unpublished.

[30] Y. Ajiro et. al. private communication.

[31] T. Nishikawa, M. Kato, M. Kanada, T. Fukamachi, K. Kodama, H. Harashima, and M. Sato: J. Phys. Soc. Jpn. **67** (1998) 1988-1993.

[32] T. Fukamachi, Y. Kobayashi, M. Kanada, M. Kasai, Y. Yashui and M. Sato: J. Phys. Soc. Jpn. **67** (1988) 2107-2111.

[33] I. Affleck, T. Kennedy, E. H. Lieb and H. Tasaki: Commun. Math. Phys. **115**(1998) 477-528.

[34] T. Kennedy and H. Tasaki: Phys. Rev. **B 45**(1992) 304.

[35] S. Hill, J. A. A. J. Perenboom, N. S. Dalal, T. Hathaway, T. Stalcup and J.S. Brooks: Phys. Rev. Lett. **80** (1998) 2453.

[36] R. E. Dietz, F. R. Merritt, R. Dingle, D. Hone, B. G. Silbernagel and R. M. Richards: Phys. Rev. Lett. **26** (1971) 1186.

[37] T. T. Cheung, Z. G. Soos, R. E. Dietz and F. R. Merritt: Phys. Rev. B**17** (1978) 1266.

[38] T. Tonegawa,T. Hikihara, M. Kaburagi, T. Nishino, S. Miyashita and H.-J. Mikeska: J. Phys. Soc. Jpn. **67** (1998) 1000.

[39] R. Kubo, M. Toda and N. Hashitsume: *Statistical Physics* II, (Springer-Verlag,Berlin 1978).

[40] S. Hill, J. A. A. J. Perenboom, N. S. Dalal, T. Hathaway, T. Stalcup and J.S. Brooks: Phys. Rev. Lett. **80** (1998) 2453.

[41] K. Katsumata, J. Magn. Magn. Matter. **140-144** (1995) 1595.